POLITECNICO
MILANO 1863

Evaluating Mechanical and Thermal Properties of MDO PE and BOPP Films for Enhanced Food Packaging Performance

MASTER THESIS IN FOOD ENGINEERING

Author: **Michael Zocca**

Student ID: 10537908

Academic tutor: Prof. Luigi De Nardo

Company tutor: Ing. Luca Morato

Academic year 2022/2023

[I got new rules, I count 'em]

Abstract

The thesis conducted at Goglio S.p.A. and the Politecnico di Milano focused on the mechanical properties, particularly Young's modulus, of Machine Direction Oriented Polyethylene (MDO PE) and Biaxially Oriented Polypropylene (BOPP) films, which are essential in the packaging industry, especially in multilayer packaging solutions. The research primarily aimed to understand the materials' behaviour under different temperatures and stresses during the production process, with a special focus on the machine direction, which is crucial for maintaining product quality and integrity. The study involved conducting tensile tests on various films, including five types of MDO PE from different suppliers and a BOPP film already in use. These tests were critical in evaluating how these materials behave when subjected to the stresses of production. Adhering to the ASTM D882 – 10 standard for tensile testing of thin plastic films, the tests were performed at different temperatures (24, 30, 60, 80°C) considering factors like the target temperature in various parts of the drying tunnel and the fusion point of each material as indicated by Differential Scanning Calorimetry (DSC) results. A key finding was the variation in mechanical properties among different MDO PE films. This variability emphasizes the importance of comprehensive testing and supplier selection for specific packaging needs. The exponential model for Young's modulus in the thesis demonstrates a strong correlation (R-squared > 0.98) between the modulus and temperature, indicating that elasticity changes significantly with temperature (for MDO PE and BOPP in machine direction). Furthermore, laboratory analysis has identified a linear correspondence (R-squared > 0.98) between specific heat capacity and temperature in the operative range of 20-100°C. This has led to the development of linear models to predict the change in specific heat at the operating temperatures of the drying tunnel.

KEY WORDS:

MDO PE, BOPP, tensile test, elastic module , packaging, laminate, solvent

Sommario

La tesi condotta presso Goglio S.p.A. e il Politecnico di Milano si è concentrata sulle proprietà meccaniche, in particolare sul modulo di Young, dei film di polietilene orientato in direzione di macchina (MDO PE) e di polipropilene orientato biassialmente (BOPP), essenziali nell'industria del packaging, soprattutto nelle soluzioni di imballaggio multistrato. La ricerca mirava principalmente a comprendere il comportamento dei materiali a diverse temperature e sforzi durante il processo di produzione, con particolare attenzione alla direzione MD, che è cruciale per mantenere la qualità e l'integrità del prodotto. Lo studio ha comportato l'esecuzione di prove di trazione su vari film, tra cui cinque tipi di MDO PE di diversi fornitori e un film BOPP già in uso. Questi test sono stati fondamentali per valutare il comportamento di questi materiali quando sottoposti a sforzi durante la produzione. In conformità allo standard ASTM D882-10 per le prove di trazione di film plastici sottili, i test sono stati eseguiti a diverse temperature (24, 30, 60, 80°C), tenendo conto di fattori quali la temperatura target in varie parti del tunnel di evaporazione solvente e il punto di fusione di ciascun materiale, come indicato dai risultati della calorimetria a scansione differenziale (DSC). Un dato fondamentale è stata la variazione delle proprietà meccaniche tra i diversi film di MDO PE. Questa variabilità sottolinea l'importanza di test completi e della selezione dei fornitori per le specifiche esigenze di imballaggio. Il modello esponenziale per il modulo di Young nella tesi dimostra una forte correlazione (R-quadrato > 0,98) tra il modulo e la temperatura, indicando che l'elasticità cambia significativamente con la temperatura (per MDO PE e BOPP in direzione MD). Inoltre, l'analisi di laboratorio ha individuato una corrispondenza lineare (R-quadro > 0,98) tra la capacità termica specifica e la temperatura nell'intervallo operativo di 20-100°C. Ciò ha portato allo sviluppo di modelli lineari per prevedere la variazione del calore specifico alle temperature operative del tunnel di evaporazione solvente.

PAROLE CHIAVE:

MDO PE, BOPP, modulo elastico, imballaggio, laminate, solvente

Table of Contents

Introduction of the Company

Goglio S.p.A. is an Italian company specializing in packaging solutions, particularly in flexible packaging and packaging machinery. It has a long history dating back to its founding in the early 20th century and today is still led by the Goglio family under the vision of President Franco Goglio.

Goglio was founded in 1850 in Rho (MI), in the north of Italy more specifically in Lombardy, by the Goglio family. During the early 20th century, the company began its journey into the world of packaging.

In the 1960s and 1970s, Goglio expanded its operations and started investing heavily in research and development. This period of growth saw the company develop and introduce various innovative packaging solutions, including flexible packaging for food products, which was becoming increasingly popular due to its convenience and cost-effectiveness.

It's noteworthy to mention that back in 1968, Goglio introduced and secured a patent for the unidirectional degassing valve. As the years passed, this innovation became the standard choice for packaging freshly ground or whole-bean coffee among major coffee roasters worldwide. Consequently, Goglio now manufactures over a billion of these valves each year on a global scale.

Goglio continued to expand its reach during the 1980s and 1990s. They expanded their product range and began establishing a global presence by opening subsidiaries and production facilities in different parts of the world such as the USA, Spain, and the Netherlands. This move allowed them to serve international customers better.

In the years 2000s Goglio continued to innovate and diversify its product offerings. They focused on sustainable packaging solutions, including the development of materials that were more environmentally friendly. This aligns with the global trend of increased awareness of the environmental impact of packaging materials [1].

Goglio produces flexible packaging solutions such as bags and pouches. These can be used for various food products, including coffee, snacks, pet food, and more. Goglio

is known for its expertise in coffee packaging, offering solutions like coffee valve bags that help preserve the freshness of coffee beans and ground coffee.

Figure 1 Example of Goglio packaging used for coffee beans where it's present the valve bags [2]

Goglio is a company that specializes in producing high-barrier laminates. They offer these laminates in various types of formats including vacuum packs, soft packs, stand-up bags, and industrial bags on reels (FFS). One of their greatest achievements is the FRES-CO ASEPTIC SYSTEM®, which allows products to be processed and kept at room temperature without preservatives. This system helps to maintain the taste, nutritional value, and organoleptic properties of the products for a much longer period of time. Apart from packaging, Goglio also provides packaging machinery and services using hot fill, cold fill, vacuum, and aseptic technology [2].

The company in 2021 has generated 395 million in revenue most of which is coming from the coffee sector. In the figure 3 is it possible to visually understand the market sector in which Goglio generates more revenue. it is easy to see that the company is closely linked to the food sector not only through the coffee industry but also through the aseptic system (mostly used for tomato sauce) and other food-related packaging [3].

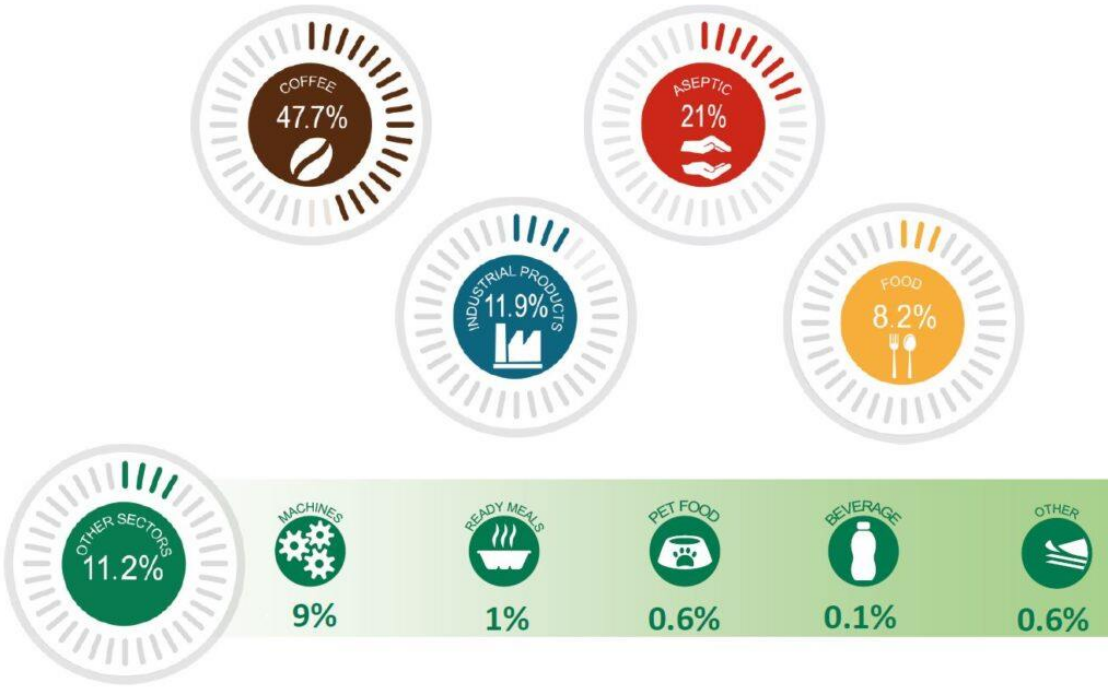

Figure 3 Goglio's revenue for 2021 divided by market sector [3]

Goglio's global presence, with eight plants located in Italy, the Netherlands, China, and the USA, has made these results possible. North America is the largest market by geographical area, contributing almost one-third of the total revenue as shown in figure 5.

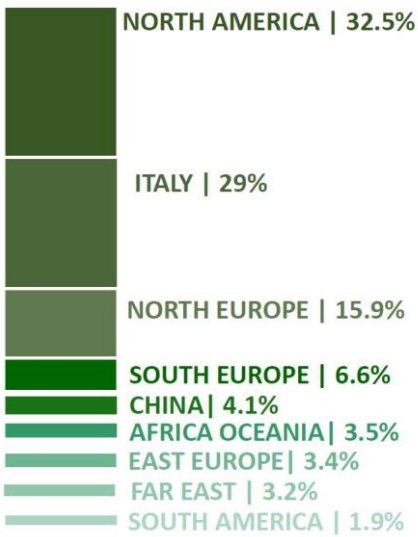

Figure 5 Goglio's revenue for 2021 by geographical area [3]

The company strongly promotes cross-divisional interaction and cooperation, facilitating a collaborative approach to identifying and pre-empting growth opportunities in each country. This exchange of knowledge and expertise empowers Goglio to respond more effectively to the demands and evolving dynamics of the global market. Keeping that in mind the biggest plat is still located in Daverio (VA) where place where the internship took place [3].

Figure 6 Goglio's headquarters in Daverio (VA) drone POV

1 Organization of internship and extra Thesis activities

The internship at Goglio S.p.A. occurred at the Daverio (VA) production site, starting in early March and lasting for a full six months, from Monday to Friday, with working hours from 8 a.m. to 5 p.m., constituting a full-time commitment. Throughout the internship, the primary focus was on conducting research for the thesis. This endeavor made optimal use of the company's collective knowledge and the quality control machinery and rotogravure equipment available in the converting department of the plant.

It’s important to say that certain activities, particularly high-temperature tensile strength tests, were conducted in the laboratories at the Mancinelli Campus (Politecnico di Milano) during June and July. This was necessary because the specific equipment required for these tests was hard/time-consuming to set up at the company so would affect negatively the output of the Quality Control department.

It's worth highlighting that during the internship, an opportunity emerged to enhance certain aspects of the converting department, with guidance from Tutor Luca Morato and Converting Supervisor Roberto LaRosa. One specific issue addressed the storage of spare parts for the Cerutti A0570 rotogravure machine.

This machine has components that require periodic cleaning due to the accumulation of excessive adhesive on them. To tackle this challenge, multiple sets of these components were in use, allowing one set to be cleaned while another set, or more, was utilized to keep the machine running. However, the problem existed because there was no organized storage system for the freshly cleaned parts while they awaited their turn to be used.

The components in question included:

- Blades whose purpose is to remove excess adhesive
- Injector cover
- Under blades
- Blade guards
- Lateral cover
- Adhesive drains
- Injector hoses
- Injector Nozzles

The task was to find an efficient solution for the storage of these components efficiently according to LEAN visualization management. The aim was to have a custom-made compact storage system where everything has its place and nothing else can be put in the wrong spot, while at the same time being able to easily check if a piece is missing simply by looking at the structure, without having to open/search for anything.

The initial process involved cataloging all the machine parts and determining which parts needed to be included and in what quantity. After that, the fundamental dimensions of the components were obtained in order to digitally reconstruct them using Shapr 3D modeling software. This was done to ensure that the fundamental specifications of the components were accurately captured and that the resulting digital models were true to the physical components.

After defining the maximum area that the storage system could occupy, a preliminary design was proposed and refined through several iterations. Dimensions and position of the entire storage system were checked before construction using Apple augmented reality kit® to make sure that everything would fit perfectly in the space allocated and that there was enough space for the operators to do their jobs comfortably.

The final design in figure 10 was chosen.

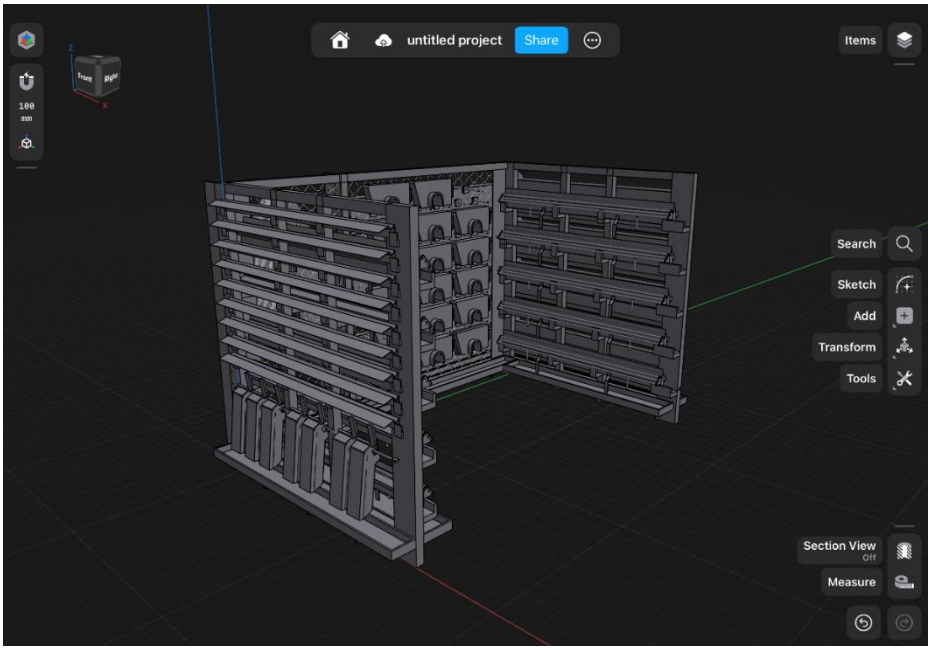

Figure 10 Final design storage system for Cerutti A0570

After that came the construction phase, which was entrusted to a locksmith from outside the company. The final result after painting is as in figure 11.

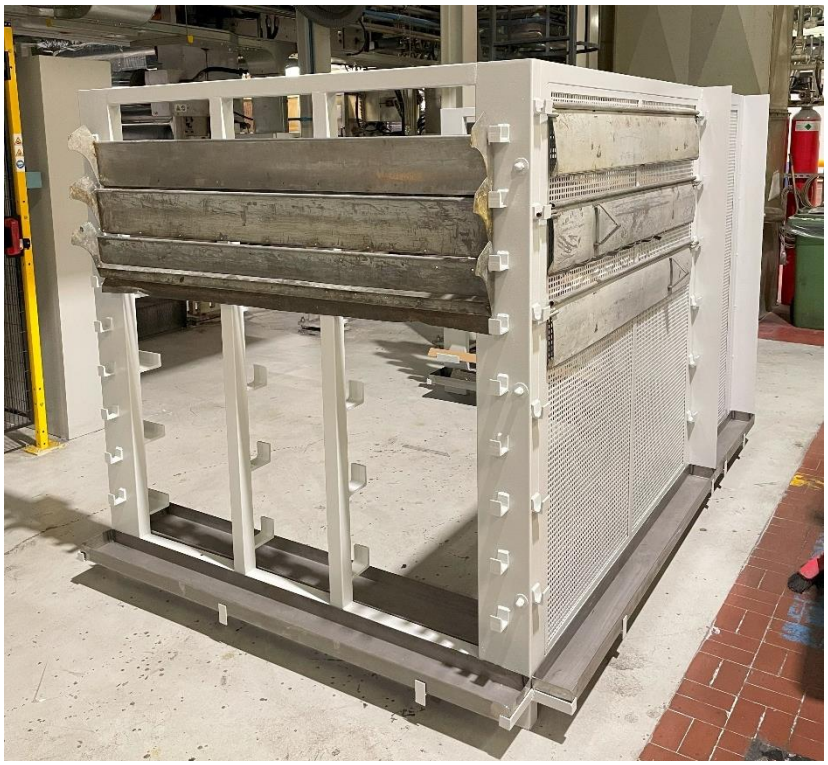

Figure 11 Storage system built with some components already on it

In addition, during the internship period, it was possible to assign spaces for the new work area used for the Supersimplex machine. The main objective was to determine what should be placed, how much floor space it takes out, and where to place it in order to have a well-organized area minimizing the travel space from the idle position to the work position and, at the same time, being easily accessible to workers and handling vehicles. Specifically, the necessary equipment consists of:

- Mixer
- 220L adhesive tank
- 220L catalyst tank
- 2 structures for storing the nip rollers
- trolley to remove the nip rollers
- shelves
- culler for the treater

A part of the area should also be assigned to the storage of reels waiting to be used.

After some iteration, the design was chosen as in figure 15.

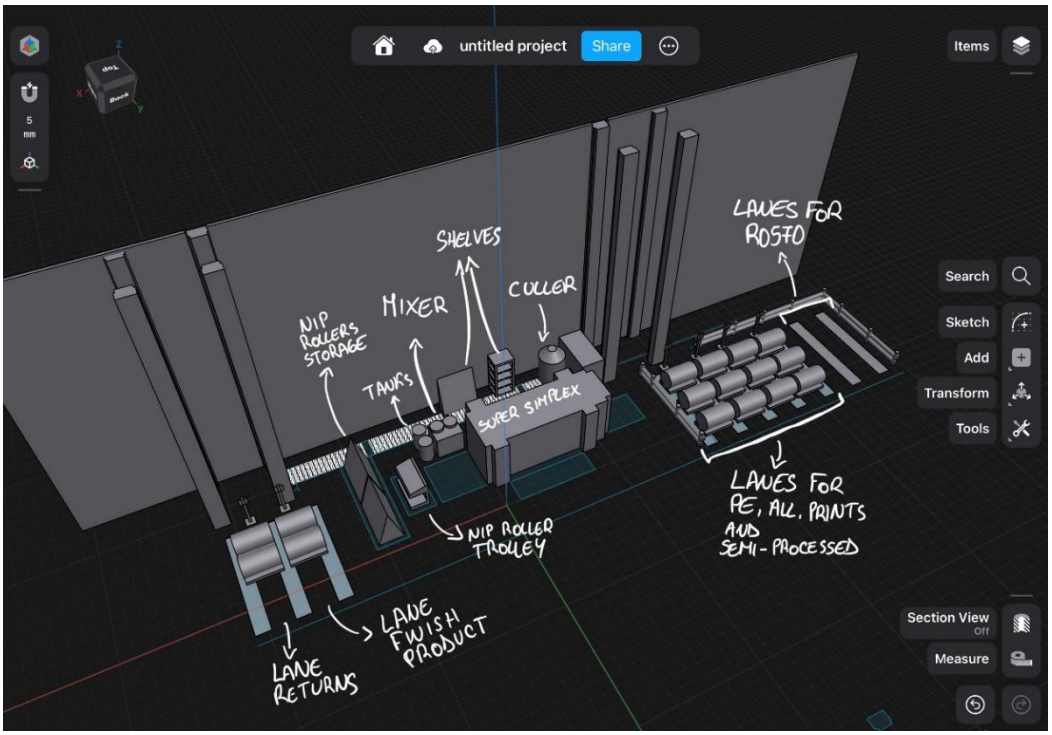

Figure 15 Final design for the Simplex machine and storage of reels

In the image, it's possible to see a 3D reconstruction of the fundamental dimension of the equipment paying special attention to the floor space occupied. Nip rollers have been positioned close to the adhesive spreader, alongside the mixer and adhesive and catalyst tanks. Clear delineation has been made for both operational and trolley pick-up areas for the nip rollers. Attention has been devoted to ensuring the smooth passage of operators with the trolley during their work.

The waiting reel stationing area, on the other hand, has been designated on the opposing side, adjacent to one of the two unwinders. The rationale behind the reel stationing arrangement involves the allocation of one lane for each major material group (such as PE, Aluminium, reels from the printing department, and semi-finished products) guard rails have been added to guarantee the safety of the operator. The remaining two lanes have been reserved for the reel stationing of R0570.

To facilitate the handling of finished products and returns, two separate lanes have been designated, ensuring that forklift operators can access them without interrupting those involved in the delivery of materials for lamination.

To prevent forklift operators from pushing the baskets on the floor, which would wear and ruin the floor, the idea of using thin steel plates to support the basket feet was proposed (not yet adopted). Plates thin enough to allow forklift wheels to climb on without wearing out the wheels, and spaced far enough apart (1m) so that the pallet truck could be used to move the reels from the lane to the machine and vice versa.

In figure 16 it's possible to see the space in setup, yet not finished.

Figure 16 Space in setup dedicated to Supersimplex machine

2 Description of the problem

2.1 Objective of the Thesis

The objective of the thesis is to determine the mechanical properties, particularly the elastic modulus, of plastic films focusing on MDO (machine-direction oriented) PE (polypropylene) films, at different operating temperatures within the plant. The goal is to establish a range of energy per unit area [J/m^2] that can be applied to the film during the solvent removal phase in the **drying tunnel** compatible with the desired solvent retention and the tension needed on the film during production to guarantee the quality of the final product. This will ensure that the plastic material is acceptably deformed in the machine direction following production quality standards. The MDO PE layer is supposed to be used in a multilayer packaging solution.

2.2 Description of the Packaging Solutions

Goglio excels in the production of a wide array of flexible packaging solutions designed to cater to the distinct requirements of diverse industries. One notable sector in which Goglio thrives is the coffee industry, with esteemed clients like Lavazza. The necessity for multilayer packaging within this domain stems from an intricate interplay of factors, all converging to ensure the utmost quality and preservation of the cherished coffee product or food matrix in general

One primary consideration in crafting multilayer packaging is the demand for specific mechanical characteristics. Coffee for example, whether it's in whole bean or ground form, requires packaging that can withstand various challenges it might encounter during its journey from production to consumption. These challenges can range from resistance to tearing and abrasion to the ability to endure the stress induced by vacuum packaging processes. Ground coffee, in particular, is often subject to rigorous vacuum sealing, which necessitates packaging that can withstand such mechanical forces.

Goglio S.p.A. also offers different shapes of packaging from soft packs to stand packs to industrial packs that have to carry a lot more weight than the normal supermarket bag.

However, beyond these mechanical attributes, the preservation of the coffee product itself is of paramount importance. To achieve this, one crucial parameter is the OTR, or oxygen transmission rate. This measure signifies the quantity of oxygen that can permeate a packaging substrate within a specific time frame. In the case of coffee, maintaining an optimal internal environment is critical to prevent oxidation, a process that could severely deteriorate the nutritional and sensory qualities of the coffee. Thus, controlling the OTR within the packaging is vital in ensuring the product's longevity and quality [4].

Moreover, practical requirements add to the complexity of designing multilayer packaging. One such requirement involves the ease of sealing the bag made from this specialized plastic material. The ability to securely seal the bag without causing any damage to the remaining portion is essential for both the end consumer and the producers. Other requirements can be to withstand higher temperatures than 105°C for pasteurization [5] of the food matrix or an easy printable surface.

To put it simply, multilayer packaging emerges as the perfect solution due to its unique ability to blend the distinct characteristics of various materials into a singular flexible packaging solution. Each layer of the final packaging solution provides the solution for just one or more problems listed above.

In figure 17 there's an example of a 3 layer-laminated sheet with Polyethylene as the inner layer which is great for welding the bag, EVOH as the intermediate layer creating a barrier for oxygen and PP as the external layer:

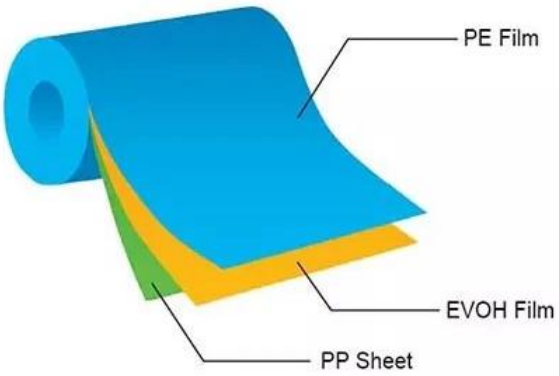

Figure 17 Example of a 3-layer laminated sheet with Polyethylene as the inner layer, EVOH as the intermediate layer creating a barrier for oxygen and PP as the external layer [28]

In recent years, special emphasis has been placed on sustainability, and great efforts have been made to improve this aspect. Precisely for this reason, efforts are being made to migrate toward a type of packaging composed of multiple layers of the same resin, as in the case of Goglio S.p.A., which presented mono-material products such as mono-PE or mono-PP packaging at interpack 2023 in Düsseldorf [6]. The advantage of this type of approach is the possibility of being able to recycle the mono-material bag and recover it, where applicable, in existing waste management facilities. The goal of this thesis is also to be able to provide new data regarding the change in mechanical properties (of which knowledge is essential to operate production machines) under different temperature conditions. More specifically PE MDO is a polyethylene film heated to a temperature slightly below its melting point and stretched in a particular orientation, machine direction in this case, to improve its mechanical properties [7].

2.3 Description of the adhesive

Understanding the materials used in multi-laminated flexible packaging is just as crucial as understanding the different technologies used to bond the layers together. This is because each technology requires specific production steps that the material must undergo to create the final product. These steps involve changes in the operating temperature, pressure, and mechanical stress applied to the film.

The most commonly used approaches in the industry are:

- Thermolamination
- Solventless Adhesives
- Water Based Adhesives
- Solvent Based Adhesives

Thermolamination is the process of adhesion between two layers by applying only temperature and pressure without using adhesives [8]. The specific conditions of temperature and pressure are obtained through the use of heated calenders. The final result is two or more layer that seems fused together.

Solventless lamination as the name suggests consists of using adhesive without organic solvents or water as carriers. Usually, the adhesive is mixed with a catalyst (in certain weight ratios) before the compound is fed into the machine. Also in this situation, it is important to control the temperature at which the mix is being fed and the single temperature of the adhesive and catalyst before the mixing (as well as ensuring proper mixing using mixing nozzles). Since the use of the adhesive is vital, it is extremely important to apply exactly the required amount to the plastic substrate otherwise, problems with derailment of the reels or poor adhesion between substrates

can occur. In figure 18 is possible to visually understand how the adhesive is spread on the film.

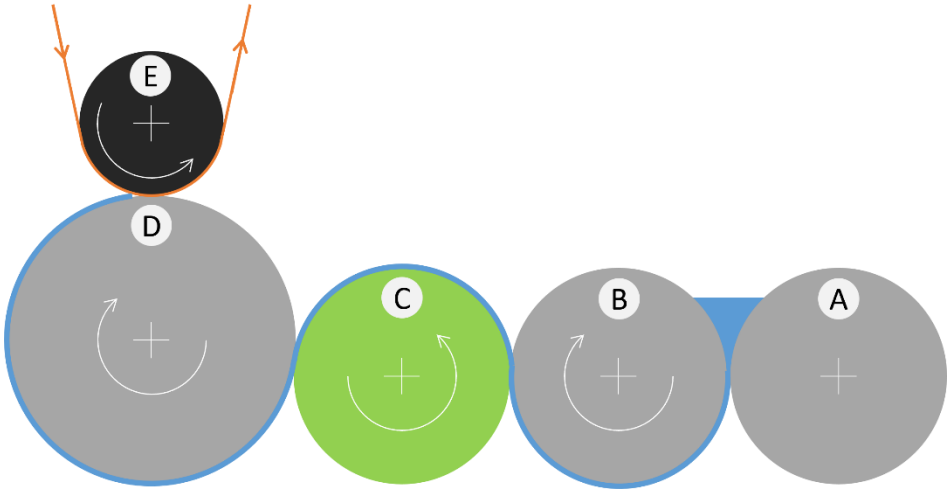

Figure 18 How flow of adhesive mixed with catalyst is adjusted and spread on the plastic film [9]

As guessed from the image the distance between roller A-B and the speed of roller C (rubberized roller carrier) can be acted upon to adjust the amount of adhesive. The speed of roller D is the same as the line speed (ensuring the necessary tension on the film) while that of roller B is always kept at about 1/3 of that of C [9]. Solventless lamination adhesives allow packaging converters to save costs by eliminating the need to use ovens to remove water or solvent carriers in water-based or solvent-based adhesives.

Solvent-based adhesive systems typically consist of a polymer, a crosslinking agent, and sometimes functional additives. The role of these additional components is to give specific functional characteristics and to modify the performance of the adhesive.

A solvent is introduced, during the preparation of the adhesive, into the base polymer in order to adjust its viscosity [10]. Unlike solventless technology, there is no roller carrier but rather an engraved cylinder that can directly "catch" the adhesive or colour (because remember that even in the printing department they use solvent for rotogravure production) from a basin below.

Figure 19 shows how the spreader works:

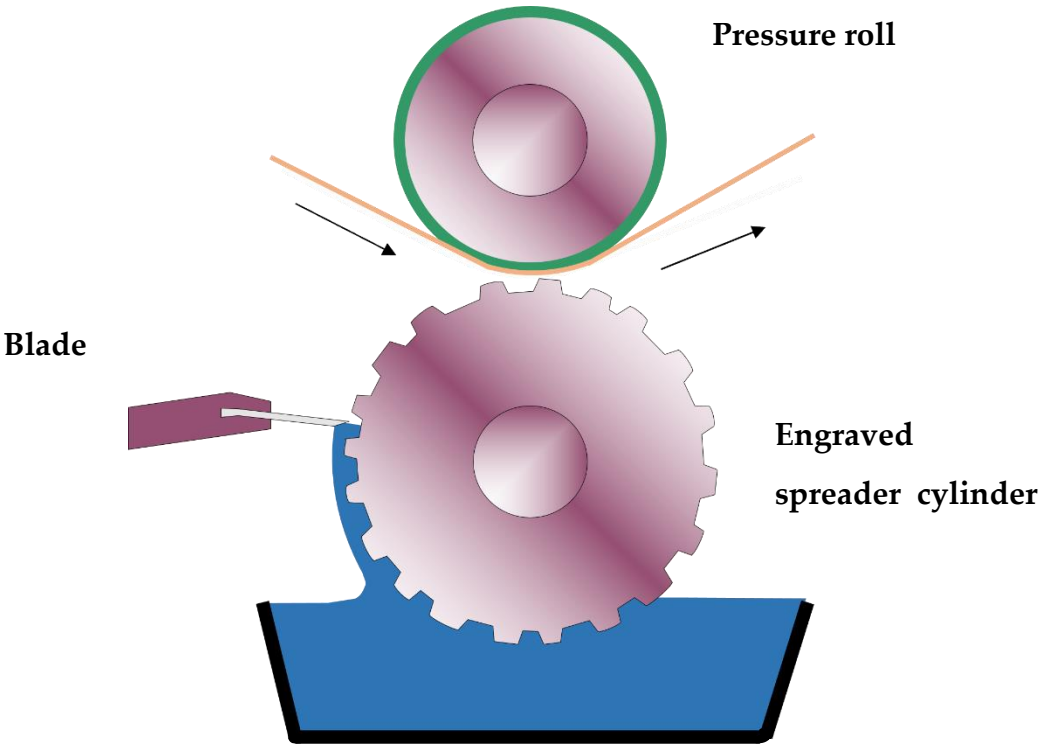

Figure 19 Representation of a spreader [9]

The pressure roll, made of rubber, applies even pressure to the film against the metal cylinder. Its high coefficient of friction and hardness can be changed by simply changing the formulation of the rubber [11]. The aim is to have an adhesive that can be easily spread on the film. Viscosity and, as a result, the concentration of solvent in the adhesive plays an extremely important role in adjusting the amount of adhesive spread on the film, along with the type of engraving on the spreader cylinder. A blade is used to stop all excess solvent in fact the position, the angle, and the pressure influence the amount of solvent removed.

Higher viscosity means more adhesive and less solvent. Ethyl acetate is the major solvent used in the Goglio's plant in Daverio for both lamination and printing. It is a solvent that has a high vapor pressure so it is very volatile even at room temperature with an evaporation temperature of 77°C [12], in fact, you can smell it in the air when it is used in production. These types of adhesives, however, have the disadvantage of requiring the utilization of a drying tunnel to evaporate much of the solvent in order to ensure solvent retention (solvent concentration in the finished product) below $20\frac{mg}{m^2}$ [9]. Too high a solvent retention results in poor adhesion between the laminate layers with obvious bubbles on the product as well as a risk of organoleptic contamination of the product that will later come in contact with the laminate.

Similarly to solvent-based, **Water-based laminating** adhesives use a carrier for their resins, in this case water. The process is extremely similar to the solvent-based with a passage of the laminate in a drying tunnel at a higher temperature due to the higher temperature of evaporation of the water and a lower vapor pressure. Also in this case poor management of the spreader resulted in defects in the final laminate.

2.4 Important components in the converting process

In the context of a converting machine, and more specifically for combining two or more substrates, there are two main stations that mark the beginning and end of the converting process: the unwinder and the winder. The function of the unwinder is to handle the reels supplying of "raw material" to the machine that are the layers to be laminated, usually materials such as polyethylene terephthalate (PET), nylon, aluminium, polyethylene (PE), oriented polyethylene (OPE), polypropylene (PP), etc. The task of the winder, on the other hand, is to receive the processed laminated film to create one or more reels, which constitute the final product of the process or in some cases an intermediate product that will be laminated in other stages of the process. Usually, an attempt is made to avoid the last scenario because a second laminating process requires additional material handling and startup that results in a higher cost in terms of time and waste materials.

There are two distinct directions in the converting processes MD and TD. The machine direction (MD) is the primary orientation axis in the manufacturing process of materials like films and sheets. It is the direction in which the material moves or is processed as it is being created. The transverse direction (TD), often referred to as the cross-machine direction (CD), is perpendicular to the machine direction. It is the direction that is orthogonal to the primary processing direction.

In figure 23, you can see an extreme simplification of the process of converting where the film is unwound from one core and wound onto a different one:

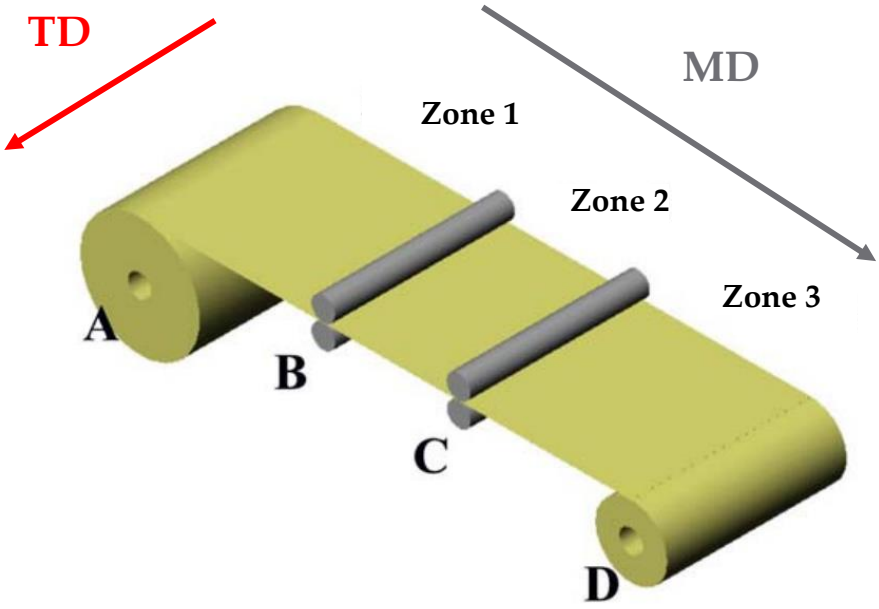

Figure 23 Unwinding (A) and winding (B) of a reel with two NIP point (B and C) and machine and transversal direction indicated [29]

From the image above it is possible to identify three different distinct tension zones to which the material is subjected. Each area is characterized by a constant tension of the material useful for the purposes of the processing to be carried out in that area. This happens because in points B and C it is possible to identify a NIP point, a point where there is contact (at certain pressures) between two rollers and where the material flows inside them. Of the two rollers that make up the NIP point, one it is motorized which allows to adjust the tension level by modulating the torque supplied to the motor and the other one is called NIP roller (usually made of rubber) which regulates the amount of pressure between the two cylinders. The winder and unwinder are also equipped with a motor and/or a pull unit capable of applying tension to the material.

Of all the NIPs in the line there is one that commands and dictates the line speed which is called the Master. All the other motors adjust to ensure the set tension, following the speed set by Master which usually turns out to be the coupler that is that part of the machine that is responsible for coupling two substrates (usually one of which is coated with adhesive) by applying pressure through a NIP roller and heat through a heated calender set to the right laminating temperature.

There are other types of rollers that operate on the line, some are simply idlers and serve only to guide the material and have no active task whatsoever, so contact with the material it's not always necessary. Others, on the other hand, have the task of changing the direction of the material, they are called "", while other rolls called "flex-curve wideners" carry out a progressive elongation of the material from the center

outward, with the purpose of eliminating creases in the material due to a spiral incision on the surface that "relaxes" the creases [9].

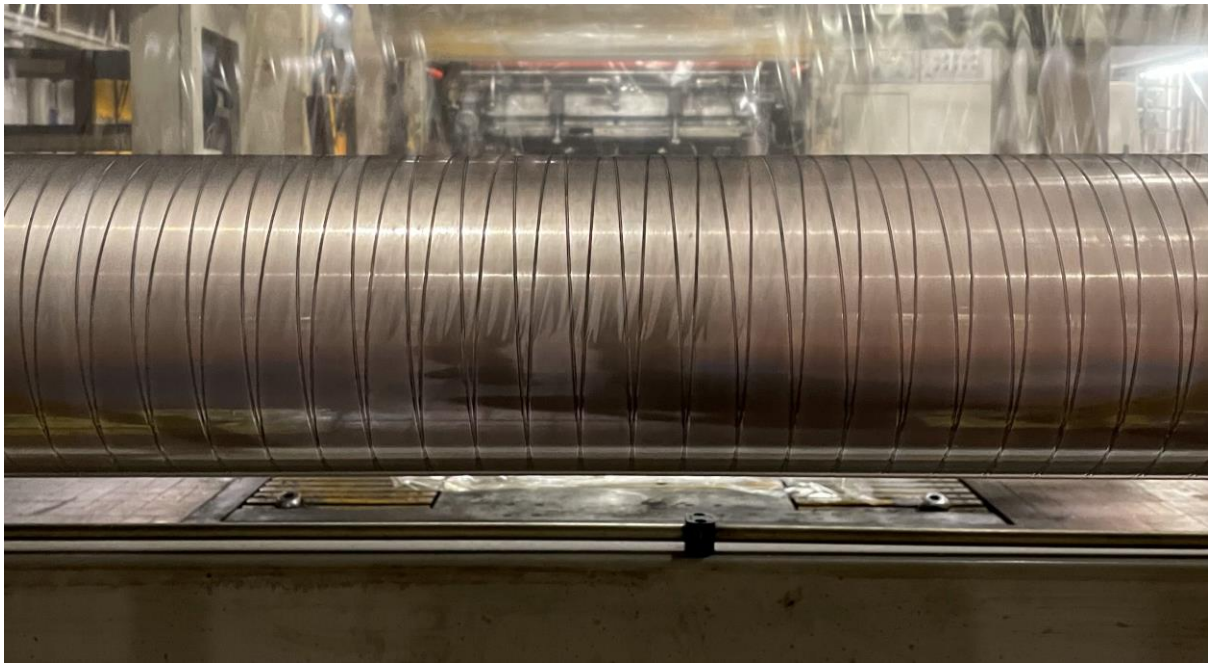

Figure 24 Example of a Flex-curve wideners in Daverio' s Plant

Finally, there is a type of cylinder whose sole purpose is to detect the tension on the material in real time and adjust the pull according to machine settings. Two different types of technologies can be distinguished in this category of cylinders:

- Load cells

- Dancers

These two different approaches although they have the same objective namely to maintain the correct film tension during processing, differ on how they go about compensating for any tension problems.

As for load cells, they are devices that allow the tensile value of the material to be obtained through the use of a potentiometer. The electrical signal is then sent to the system used to manage the tension on the material, which will adjust the NIP cylinder motors to compensate for any incorrect tension values. In figure 25, is possible to see a schematic of the forces and how the tension on the film is calculated as the wrap angle (α) changes with higher tension as the angle increases.

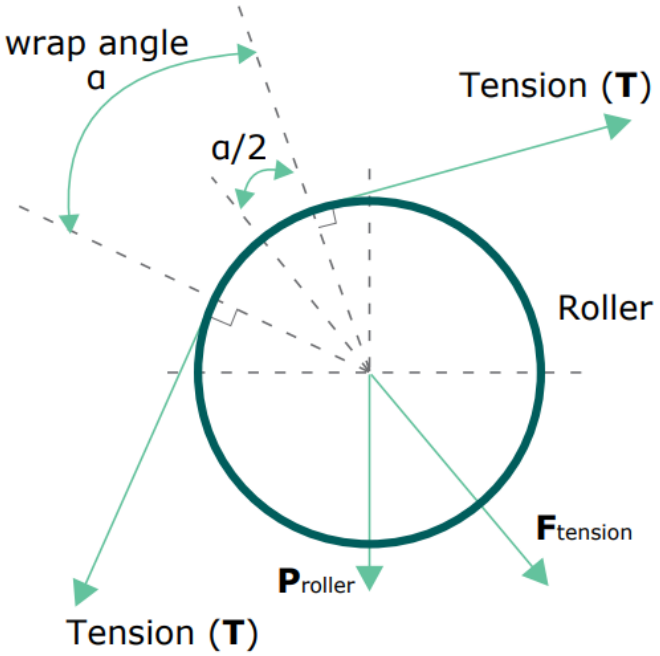

Figure 25 Schematic of the forces acting on a load cell [13]

The T is calculated [13]:

$$T = \frac{F_{tension}}{2 * \sin\frac{\alpha}{2}} \tag{2.1}$$

Where T is the force [N] related to the film tension, P_{roller} is the weight force [N] of the roller $F_{tension}$ is the force [N] result of the film tension on the roller and α the wrap angle which describes the change in direction of the film due to the contact with the roller.

From the formula above it's possible to understand that an higher wrap angle α means higher tension on the film with equal force acting on the sensor. Load cells are a good option to control tension on the film but the time needed to adjust the tension on the film can't be fast enough resulting in problems in the winding of the reel. Dancer on the other hand works in a different way and are designed to provide immediate adjustment resulting in a better option for accumulating tension spikes. A dancer consists is a passive roller with a pneumatic cylinder that adjusts its position according to the tension of the film leading [14]. In this way not only it is possible to set a desired

tension and maintain it with zero latency but it's also possible to see on the site if there is something wrong with the product just by physically looking at the position of the dancer. Figure 26 provides a schematic representation of a dancer.

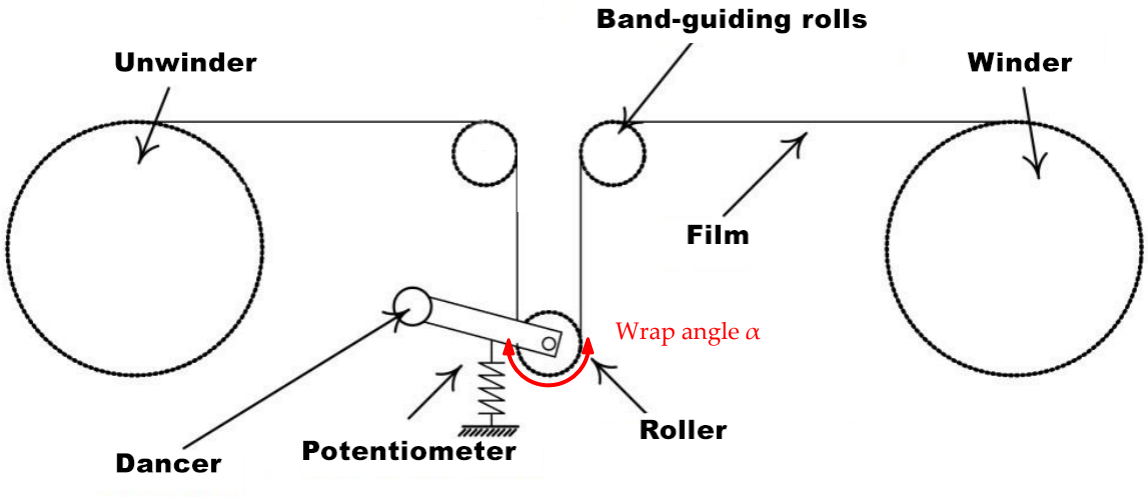

Figure 26 schematic representation of a dancer [14]

Usually dancers have a wrap angle α equal to 180° and by applying the same formula used for load cell the tension on the film is calculated:

$$T = \frac{F_{tension}}{2 * \sin\frac{\alpha}{2}} \qquad with\ \alpha = \pi \qquad T = \frac{F_{tension}}{2} \tag{2.2}$$

Therefore, it is possible to go and change the tension in individual zones by simply acting on the NIP point following it. Other types of rollers have neither the task of guiding material nor of registering tension but are used to provide extra pushing on the film at critical stages of production in converting. These "companion rollers" are equipped with a motor and are used, for example, in solvent drying tunnels where there may be a decrease in the mechanical performance of the material due to the increase in temperature.

Drying tunnels are essential to achieve the solvent retention necessary both to avoid contaminating the food matrix that will later come in contact with the finished product and to ensure adhesion between the various layers that make up the multilaminate. Temperatures inside the drying tunnels are achieved by a heat exchanger that heats

dry air by using steam at 10 bar. The air is then shot against the film 3/4 above and 1/4 to equalize the evaporation of the temperature solvent (ethyl acetate) between the top and bottom of the film. It is also extremely important to manage the oven from a safety point of view since ethyl acetate is explosive at certain concentrations. More specifically, ethyl acetate has a LEL (lower explosive limit) of 2.0 vol% and a UEL (upper explosive limit) of 12.8 vol% in air.

2.5 Analysis of the lamination process

To explore the laminating process take the A0570 machine (line M0) as an example since it is one of the most widely used lines in the Goglio plant in Daverio.

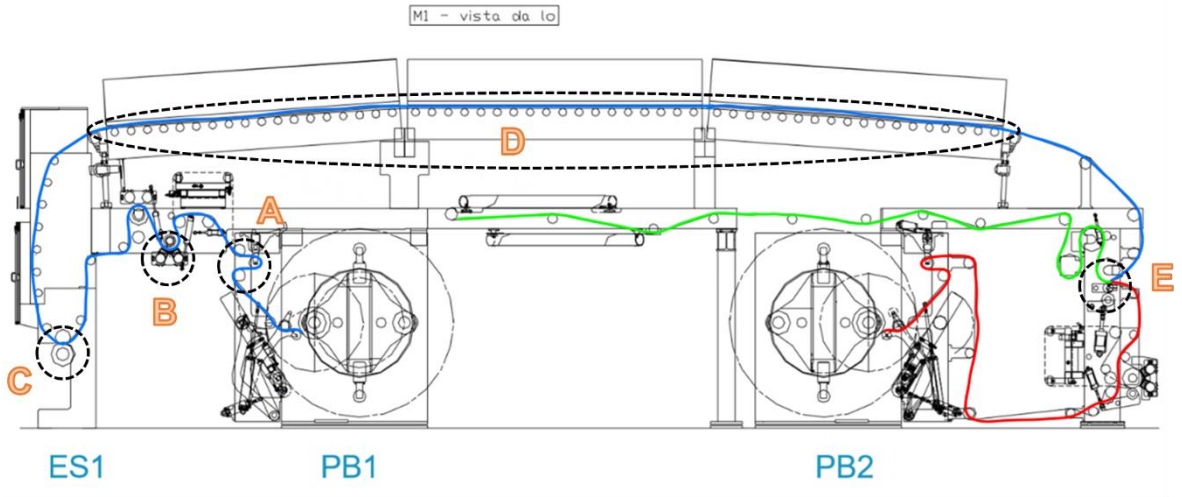

Figure 27 Figure 19 A0570 M1 line with different film highlighted in different colors [9]

From figure 27 It's possible to see, that the two films that need to be coupled start from the unwinder "PB1" and "PB2" and are coloured blue and red respectively so that they can be better tracked. The unwound film starting from the unwinder "PB1" crosses a dancer (at point A shown in the figure) which records and keeps constant tension from the unwinder to the next NIP point. After that at point B it undergoes a corona treatment process. Usually, the material has already undergone a corona treatment to increase its surface energy, making the surface more wettable and thus helping the adhesive coating process but during the lamination process this treatment is "refreshed" in line to be sure of the materials' superficial properties. Then following the material it's possible to see how at point C there is a NIP point representing the solvent-based adhesive spreader. Next, the film enters the drying tunnel which is approximately 12 meters long and consists of 3 ovens each 4 meters long. Each of these

ovens can be set with different temperatures and airflow rates, usually, it is preferred to have a slightly lower temperature in the first oven to avoid the phenomenon of blushing which consists in the formation of a "crust" on the material that would hinder the diffusion of the solvent through the film. The second oven is set at slightly higher temperatures (to evaporate as much solvent as possible) while in the third and last oven, the temperature is further decreased to avoid having the material come out at too high temperatures. To ensure optimal lamination, the temperature of the film leaving the oven must be kept as low as possible compatible with the solvent retention standards. At point E in the production line, reheated/cooled calenders will then adjust the temperature of the film to the ideal level for lamination with the second material (indicated in red). In case the exit temperature of the oven is too high, just using the heated/cooled calanders wouldn't be sufficient. Point E is also the place where lamination takes place and represents the next NIP point, so it is possible to see how the film tension through the oven can be managed between the NIPs of the spreader (point C) and laminator (point E) regardless of the other places in the line. It must be emphasized, however, how normally the tensions set in a matching line tend to gradually increase along the process, this is firstly to prepare the material for winding and secondly because during the process we get a film whose thickness increases after each rolling and which therefore requires higher tensions for processing. The final multi-layer film is then winded in another line called M2. Normally in the Daverio plant, line M1 is almost always used in combination with other lines such as M2 for the production of 3-layer packaging or again coupled with lines M2 and M0 for the production of 4-layer packaging. Other combinations with other adjacent machines such as the A0560 are also possible, and in addition, the A0570 is not the only laminating machine.

2.6 Mechanical properties of films important for the production process

During the converting process and more specifically when creating a laminated film there are several aspects of the material to be taken into consideration but Young's modulus plays a particularly important role. This is because especially in stages where a drying tunnel is present it is most important to ensure that the material does not undergo deformations beyond those tolerated. It is important to note that several materials are printed according to customer specifications so excess in deformations not only do not meet specifications and can give problems in subsequent converting stages (such as slitting and bag making) but also represent an aesthetic defect that is not tolerated. More specifically, since the material is most stressed in the MD machine direction, namely the direction in which it is pulled and dragged through the rollers,

Young's module allows to understand how much it is possible to stress the material before having a laminate that cannot pass quality control.

Young's modulus, also known as the elastic modulus, is a measure of the elasticity of a solid material. It defines the relationship between stress (force per unit area) and strain (deformation caused) in a material in the linear elasticity regime of uniaxial deformation. Young's modulus is named after the 19th-century British scientist Thomas Young. Young's module is also known as the name elastic modulus, and it gives a material's response to longitudinal stress, which is the stress applied along an axis [15]. The formula for Young's modulus E is given by:

$$E = \frac{\sigma}{\varepsilon} = \frac{\Delta\sigma}{\Delta\varepsilon} \tag{2.3}$$

where:

- σ is the stress applied to the material (force per unit area),

- ε is the strain experienced by the material (the ratio of the change in length to the original length).

Of course, $\Delta\sigma$ and the resulting $\Delta\varepsilon$ are referred to two points chosen in the linear elasticity area.

Young's modulus has the same units as pressure, which is pascals (Pa) in the International System of Units (SI). The strain ε is defined as:

$$\varepsilon = \frac{L_0}{L_0 - L_F} \tag{2.4}$$

where:

- L_0 is the initial length of the specimen.

- L_F is the final length of the specimen after the applied stress (in the linear elasticity regime).

Obviously, being a ratio between equal quantities, epsilon is dimensionless.

A high Young's modulus indicates that a material is rigid and has a high resistance to deformation under stress, while a low Young's modulus indicates that the material is flexible. An increase in humidity or temperature will generally affect in a negative way the Young's Module making the material less elastic [16]. There are ways to increase the module of elasticity such as to the alignment of the structural elements of a material, such as polymer chains, in a specific direction. This alignment can significantly increase a material's Young's modulus (E) along the orientation direction and it's done by stretching the material usually material's formation.

If stress continues past the yield stress point, the material undergoes plastic deformation, where the changes in shape remain even after the stress is no longer applied. In figure 28 is possible to see a typical stress-strain curve of a thermoplastic specimen.

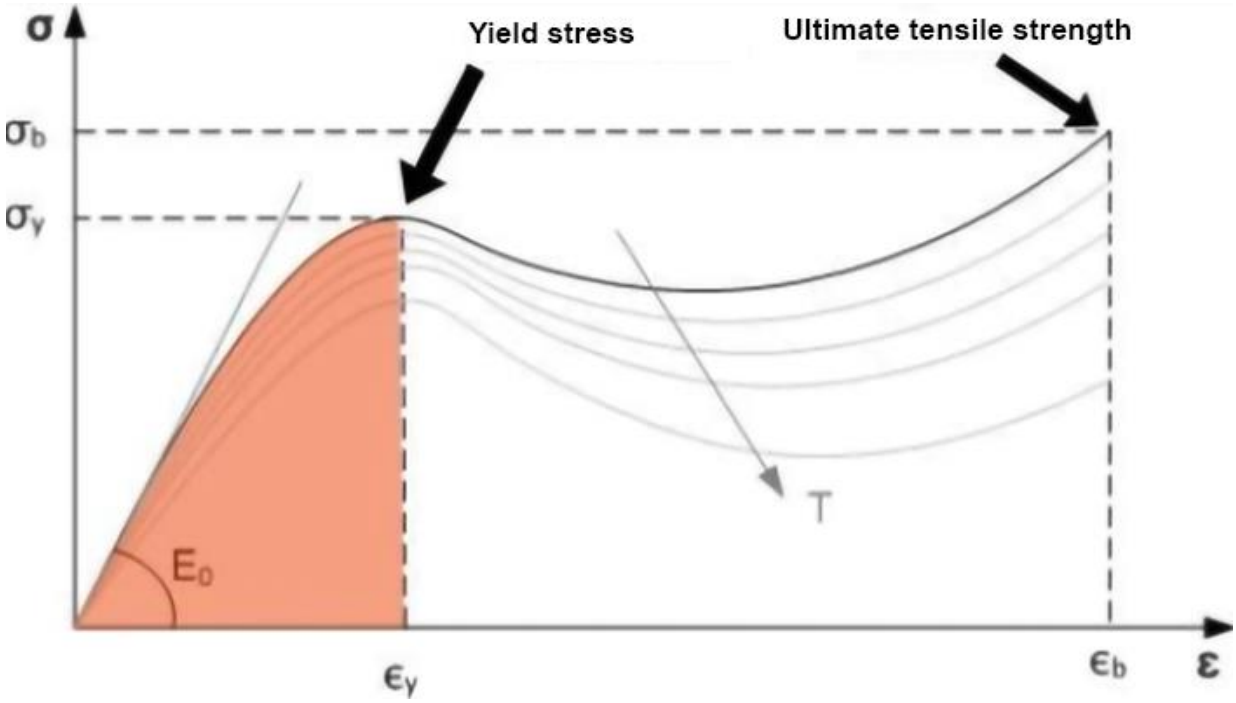

Figure 28 Typical stress-strain curve for a thermoplastic polymer

Highlighted in red the elastic region. Is it possible to see also the correlation of E with an increase in temperature (T).

Also from the strass-strain curve is possible to understand some other parameters such as resilience which refers to the energy a material can absorb and recover from

within its elastic limits (red area in the image). When the applied stress is released, the material reverts to its initial size with no lasting deformation.

Tenacity can also be quantified as the total energy a material can absorb, encompassing the elastic region, through the yielding point, and into plastic deformation. It is represented by the total area beneath the stress-strain curve during a tensile test.

3 Materials and methods

3.1 MDO PE

MDO PE film, or Machine Direction Oriented Polyethylene film, is a type of plastic film that is produced by a specialized manufacturing process to enhance its physical properties. This film is primarily made from polyethylene, a commonly used polymer in the packaging industry. PE film is primarily composed of polyethylene, which is a thermoplastic polymer. There are different types of polyethylene, each with its own set of properties. Common types used for PE films include Low-Density Polyethylene (LDPE), Linear Low-Density Polyethylene (LLDPE), and High-Density Polyethylene (HDPE). These variations offer different levels of mechanical and thermal proprieties.

MDO PE film is known for its excellent balance of properties, which makes it suitable for various applications, particularly in the packaging industry. During the manufacturing process, the MDO film is stretched in one direction (machine direction) to align and orient the polymer molecules. This results in improved mechanical and barrier properties, such as increased tensile strength, stiffness, oxygen and water vapor barrier [17] [18].

3.2 BOPP

Biaxially oriented polypropylene (BOPP) films make up the majority of biaxially oriented films, accounting for a significant portion with a global consumption exceeding 6 million tons [18]. The starting point is polypropylene polymer which is manufactured through the process of addition polymerization, which involves the connection of monomers more specifically propylene monomer, a petrochemical product in the downstream category. The film is produced using a tubular process, where a tubular bubble is inflated, or a tenter frame process, where a thick extruded sheet is heated to its softening point (not to the melting point). In both BOPP production processes, the film is then stretched in both the machine and transverse directions, resulting in molecular chain orientation in two directions. The tenter frame process typically involves stretching the film in the machine direction and in the

transverse direction by a chosen ratio, although these ratios can be adjusted as needed. This process is more common than the tubular process and yields a glossy, transparent film. Biaxial orientation enhances the film's properties, including increased tensile strength, heightened stiffness, improved clarity, enhanced resistance to water vapor and oxygen permeation. Additionally, it leads to modifications in optical properties such as a significant reduction in haze and an increase in glossiness [18].

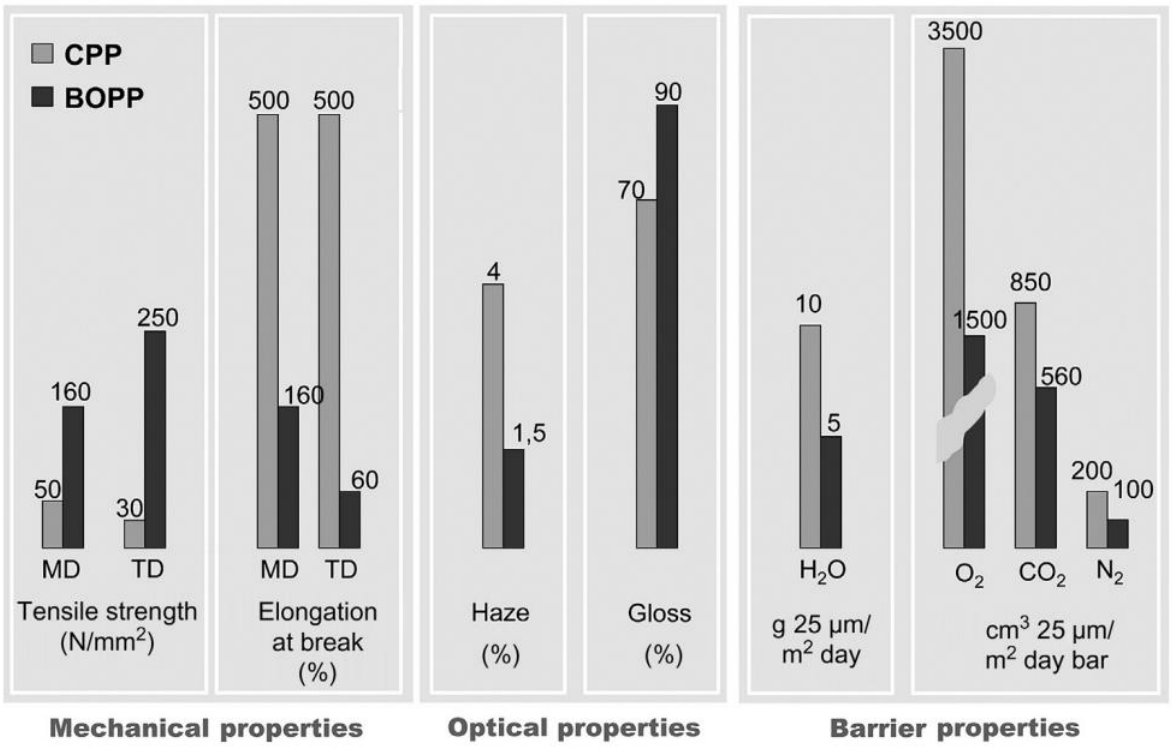

Figure 29 Property improvement for biaxially stretched PP (BOPP) versus cast PP (CPP) [18].

3.3 Specimens tested

The films tested during the internship and of interest to Goglio S.p.A. are almost all from the MDO PE class with the inclusion of a BOPP already in use at the plants. The interest in these materials stems from the desire to push the production of mono PE packaging as it is composed of a single plastic resin for all layers, allowing for better and easier recyclability of the product. This request is not simply dictated by the market and thus by consumers but also by the company's desire to offer a product with a lower environmental impact.

Considering MDO PE, it can be said that it represents a product of recent industrial development and that a standard of production has not yet been reached. This last

point leads to having different companies that offer what at first glance appears to be the same material from a different supplier when in fact the mechanical properties can vary greatly. For the testing, five MDO PEs were chosen, all coming from different suppliers with the purpose of characterizing them from a mechanical and thermal standpoint and then subsequently comparing them. The list below enumerates all five MDO PE films with the names used by the company's management software and their commercial name given by the suppliers:

- PEMDOTT supplied by Termoplast® and already used at the Daverio's plant, commercial name Crystal PE EX
- EXC21008 supplied by PolySack® and already used at the Cadorago's plant, commercial name EL DT
- EXC22004 supplied by Bluplast®, commercial code HDPE 30391
- EX23453 supplied by MG®, commercial code XXX07/05
- EXC21011 supplied by Manulitech®, commercial code MDP/PXZ

name	**code**	**thickness [μm]**	**density [g/cm³]**	**Young's modulus [MPa]**	**Yield stress [MPa]**	**Ultimate tensile strength [MPa]**	**Elongation at break [%]**
Crystal PE EX	PEMDOTT	20-25-30	0,938	>1700/>1500 MD/TD	--/>20 MD/TD	>80/>20 MD/TD	<80/<700 MD/TD
HDPE 30391	EXC22004	30 ±10%		1800/1700 ±10% MD/TD	--/29 ±10% MD/TD	120/15 ±10% MD/TD	30/300 MD/TD
XXX07/05	EX23453	27	0,94-0,96	2013 ±25%		259/36 ±25% MD/TD	38/3 ±25% MD/TD
MDP/PXZ	EXC21011	25	0,935	715	37,4/29,5 MD/TD	76,1/56 MD/TD	990/730 MD/TD
TDS Polyphane EL DT 25 μm	EXC21008	25.0 ±5%	0,94	>1000/>700 MD/TD		>100/>16 MD/TD	>25

Table 3.1 MDO PE film mechanical specification from supplier

In table 3.1, it is possible to see the most important mechanical properties such as Young's modulus and yield stress provided by the suppliers:

3.4 Standard used

All the films have been tested following the ASTM D882 – 10 standard, a widely recognized testing standard for determining the tensile properties of thin plastic films. which aims to determine the tensile properties of plastics in the form of thin sheeting and films (less than 1.0 mm (0.04 in) in thickness. Where it has not been possible to strictly adhere to the specifications, the validity and robustness of the collected data have been demonstrated [19] [20].

3.5 Selection of test temperatures

Given that the materials must pass through a drying tunnel so that the solvent can evaporate, it is important to perform not only cold tensile tests but also hot tensile tests in order to define not only the elastic modulus but also how it varies with changing temperature conditions. For this reason, tensile tests were conducted at three different temperatures for each material. The temperatures were chosen taking into account three factors:

- The target temperature of each part of the drying tunnel (especially the second one which is usually the hottest as described in Chapter 3.5)
- The Temperature of the film measured right outside the drying tunnel
- The results of Differential Scanning Calorimetry (DSC) give as output the fusion point of each material

For the **first point**, after analysing various recipes on the A0570 machine, it was possible to conclude that for some types of water-based adhesives, the maximum temperatures of the drying tunnel are set with values very close to 100°C. As for the majority of solvent-based adhesives (where the solvent is ethyl acetate), the temperatures average between 80-90°C. This is apply to the central part of the oven, which is kept at higher temperatures than the preceding and following parts, in order

to minimize solvent retention in the laminated film as much as possible without having phenomena of blushing (as extensively described in chapter 3.5)

For the **second point**, temperature measurements were taken at the exit and among the different sections of the drying tunnel, as can be seen in figure 30.

Figure 30 Exit point of the drying tunnel where temperature measurements were taken

All measurements were carried out using a certified infrared microscanner, more specifically the D501-RS Microscanner Datasheet. The measurements have shown that, on average, the temperature of the film exiting the tunnel is 20-30°C lower than the target temperature set for the air jets in the drying tunnel. This measurement allows for temperatures just above 70°C in the worst-case scenario and lower in the middle to low sixties in all other cases. The measurements also agree with the hypothesis that, since the boiling point of ethyl acetate is 77°C, the film temperature cannot reach higher temperatures because, as the solvent transitions from liquid to gas, it absorbs all the energy provided by the hot air jets. However, it must be

emphasized that the residence times in the oven are very short; at a line speed of 200 $\frac{m}{min}$ and an oven length of 12m, the residence time is only 3.6 seconds.

Finally, for the **third point**, DSC analyses were considered to establish the melting temperatures of the tested films. Employing a Differential Scanning Calorimeter (DSC) for measuring melting temperatures provides data from a system that is both calibrated and exceptionally precise. The melting point (T_m) determination via DSC reveals not just the initial melting onset (corresponding to the start of the melting process) but also the peak temperature, which signifies complete melting in the materials [21]. This method offers a wealth of information about the specimen. It is also important to take these values into account because one might be tempted to consider a worst-case scenario of 100°C or more, being a temperature value of the oven used for water-based adhesive, when in fact there are no accurate data on the actual temperature of the material inside the drying tunnels, and approaching the melting temperature of the material would lead to unusable data as if such conditions were reached in production, an acceptable result could not be obtained by definition.

On the X-axis of DSC (Differential Scanning Calorimetry) graphs for materials, you'll find temperature measured in [°C], while on the Y-axis, there is heat flow normalized [W/g]. The displayed temperature range on the graph depends on the specific material being tested and the experimental setup, typically ranging from a lower temperature to a higher temperature. The Y-axis represents heat flow or intensity, indicating the amount of heat either absorbed or released by the sample during physical or chemical changes.

In a DSC graph, peaks or valleys are commonly observed. An endothermic peak signifies a process that absorbs heat, such as melting, whereas an exothermic peak indicates a process that releases heat, such as crystallization or a chemical reaction. The melting point usually appears as an endothermic peak, characterized by a temperature increase and a decrease in heat flow. The position of the peak on the temperature axis corresponds to the melting temperature of the substance.

The beginning of the melting process is represented by the onset melting point. This point is easily identifiable because it represents a rapid increase in the heat flow values of the curve, whose peak represents, as mentioned earlier, the melting temperature.

The DSC results for all five MDO PE samples and the single BOPP sample are reported.

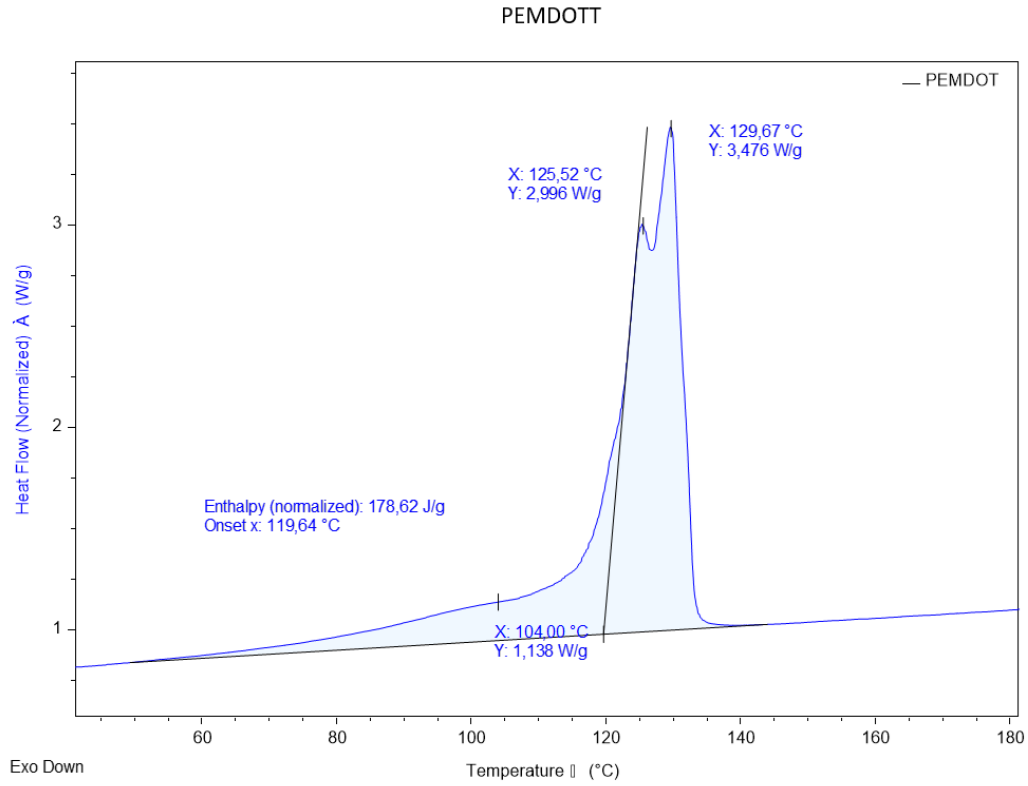

Figure 31 DSC of PEMDOTT with heat flow [W/g] as the y-axis and temperature [°C] as the x-axis

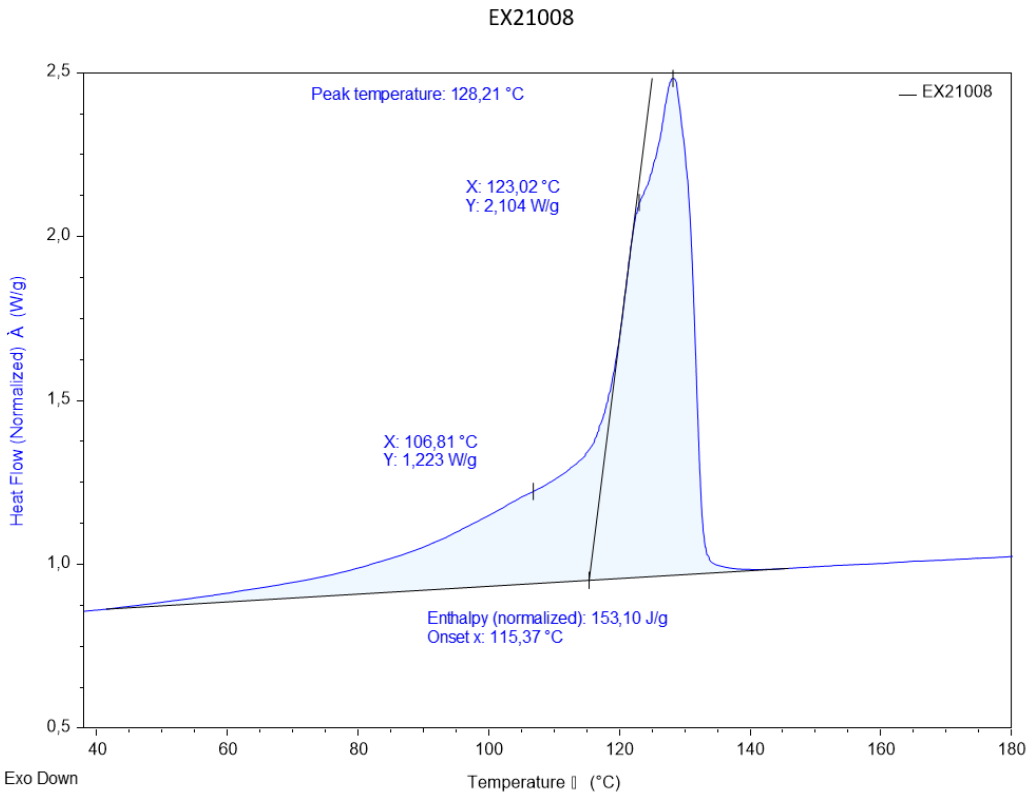

Figure 30 DSC of EX21008 with heat flow [W/g] as the y-axis and temperature [°C] as the x-axis

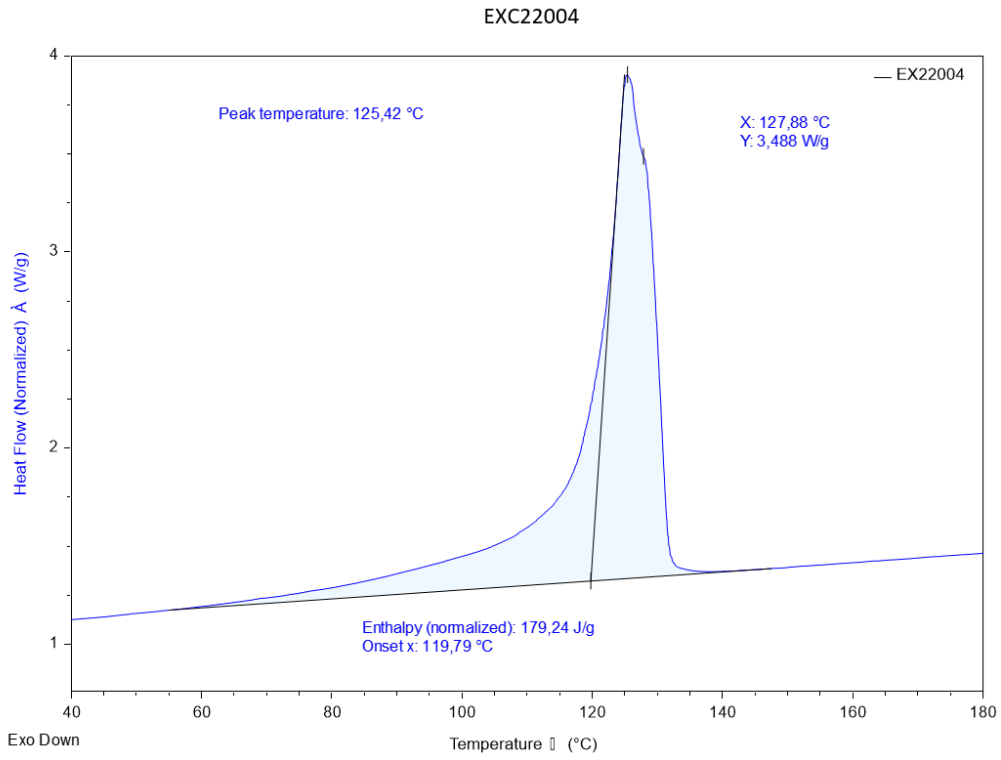

Figure 33 DSC of EXC22004 with heat flow [W/g] as the y-axis and temperature [°C] as the x-axis

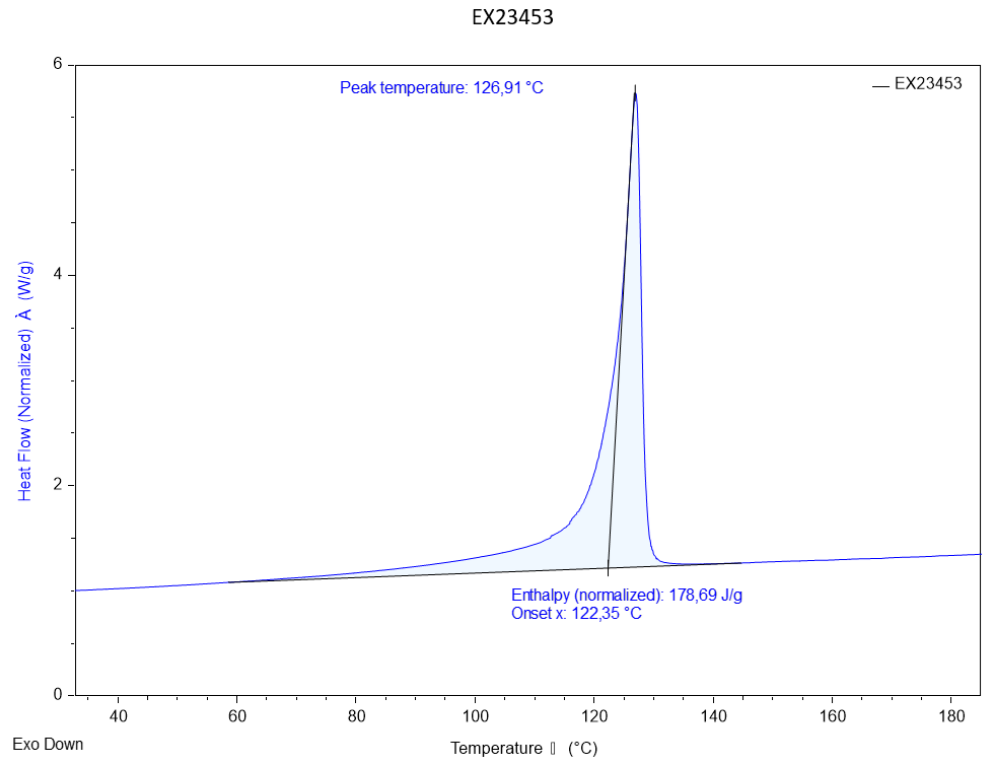

Figure 31 DSC of EX23453 with heat flow [W/g] as the y-axis and temperature [°C] as the x-axis

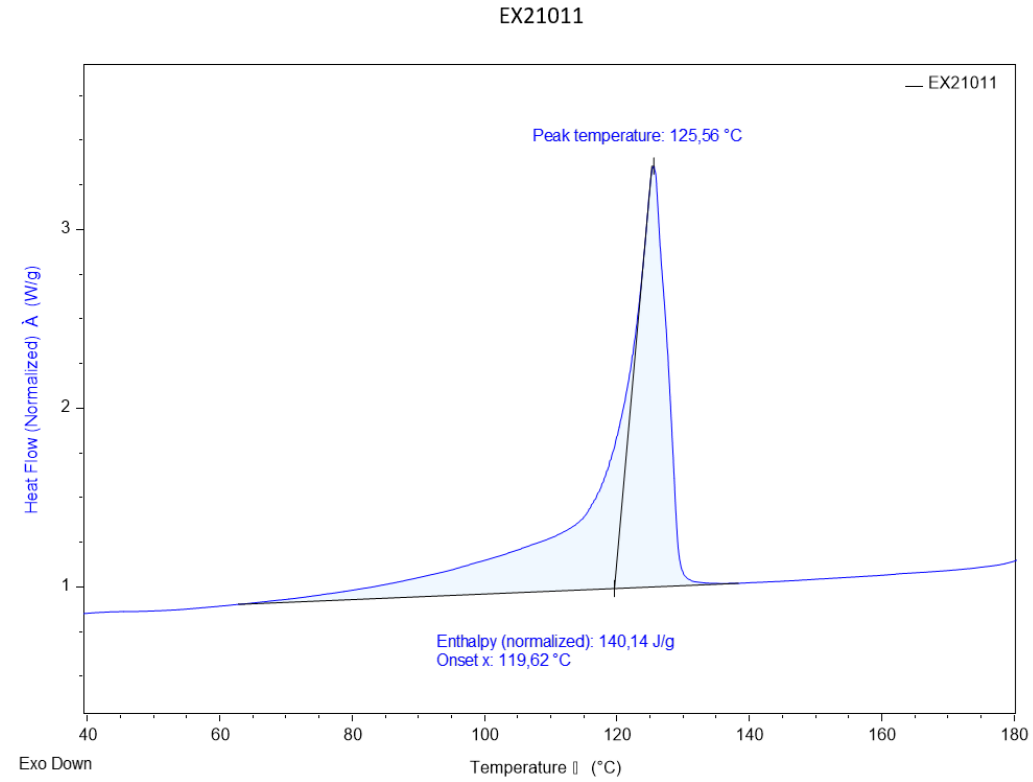

Figure 35 DSC of EX21011 with heat flow [W/g] as the y-axis and temperature [°C] as the x-axis

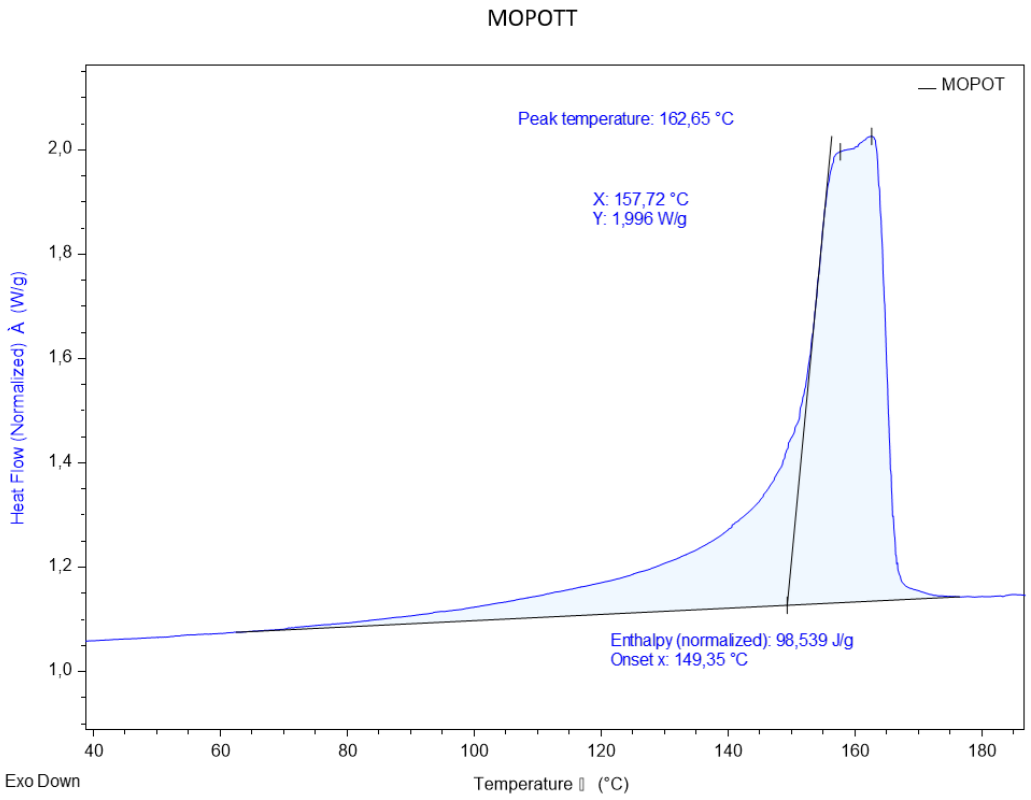

Figure 36 DSC of MOPOTT with heat flow [W/g] as the y-axis and temperature [°C] as the x-axis

Table 3.2 Melting onset values [°C] and peak melting temperatures [°C] obtained from the DSC tests of the tested materials. In blue MDO PE, in red BOPP

materials	melting onset [°C]	Peak temperature [°C]
PEMDOTT	119.64	129.67
EXC21008	115.37	128.21
EXC22004	119.79	125.42
EX23453	122.35	126.91
EX21011	119.62	125.56
MOPOTT	149.35	162.65

As can be seen from the data summarized in the table 3.2 and from the graphs in the previous pages, the melting offset point, which represents the start of the melting of the materials, is just below 120°C for all MDO PE samples, with the exception of EX23453, which is slightly above. Meanwhile, the peak temperatures, i.e., the temperatures at which melting is completed, are all in the range of 125-130°C. The results are higher for MOPOTT, which presents a melting offset point just below 150°C and a peak temperature just above 160°C. However, it is important to emphasize that by analysing the DSC graphs, one can notice a heat flow variation starting from 100°C that is not entirely negligible being close to the found value of the onset of melting.

Analyzing all the considerations explained in the previous three points, it was decided to conduct the tests at three temperatures: **30°C**, **60°C**, and **80°C**. The 30°C helps to describe the conditions in the machine (outside of the drying tunnel), considering a slight increase from room temperature due to friction between the film and the numerous rollers present. The 60°C represents an excellent middle ground for conditions near/inside the drying tunnel, while the choice of 80°C allows for examining the mechanical properties in a realistic worst-case scenario, thus reasonably far from the onset of melting temperatures of both the MDO PE and BOPP samples.

Subsequently, to the hot chamber tensile tests, another series of tests was conducted in-house at an ambient temperature of 23°C.

3.6 Test specimens

Before defining the test specimens, trials were conducted to understand the extent of elongation (especially when hot) of the materials subjected to tensile tests in both machine and transverse directions. It is important to consider this aspect since the machinery used for testing has finite dimensions and cannot accommodate every type of elongation. Following these trials, it was decided to conduct the hot tensile tests using test specimens of different dimensions from those recommended in the ASTM D882 – 10 standard. The test specimens were chosen to be in the shape of a 'dog bone' to easily identify the useful test section of the sample, which is the area between the grips of the machine that is subjected to stress and consequent elongation. In the image below, the dimensions of the 'dog bone' specimens used in the hot tests are depicted.

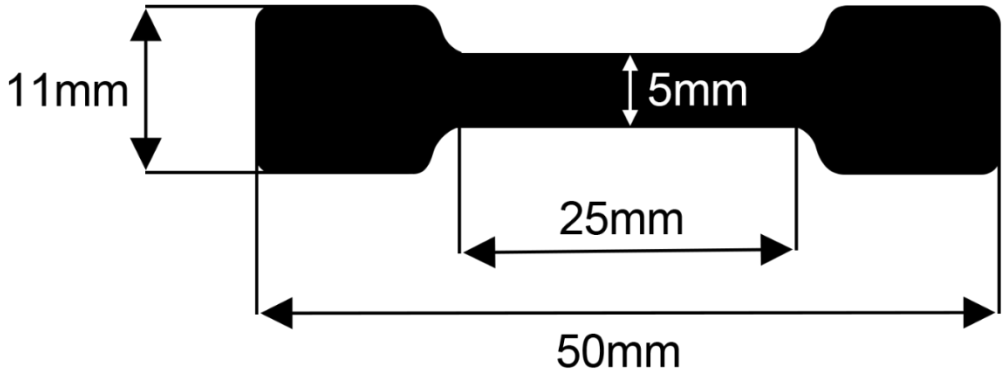

Figure 37 Dimensions of the 'dog bone' specimens used in the hot tests

As can be seen from figure 37 the dimensions of the test specimens, the useful section is 5mm in width and 25mm in length, while the dimensions including the portion of the specimen that will be gripped by the clamps are 11mm in width and 50mm in length.

In order to obtain test specimens suitable for use in tensile tests without any defects that could compromise their mechanical properties, it was necessary to produce a custom hollow cutter. Once positioned with the sharp side of the film, it was possible to obtain the desired shape specimens with a simple hammer strike. In figure 38 the custom hollow cutter.

Figure 38 Custom hollow cutter

Since the test specimens used in the hot tensile tests were different from those suggested by the reference standard, it was necessary to conduct a subsequent series of tests using dimensions conforming to the ASTM D882 – 10 standard to verify that the 'dog bone' shape of the specimen did not affect the test results. The dimensions of the tests conducted at room temperature with the standard shape consist of strips 15mm in width and a useful length of 100mm created using a cutter.

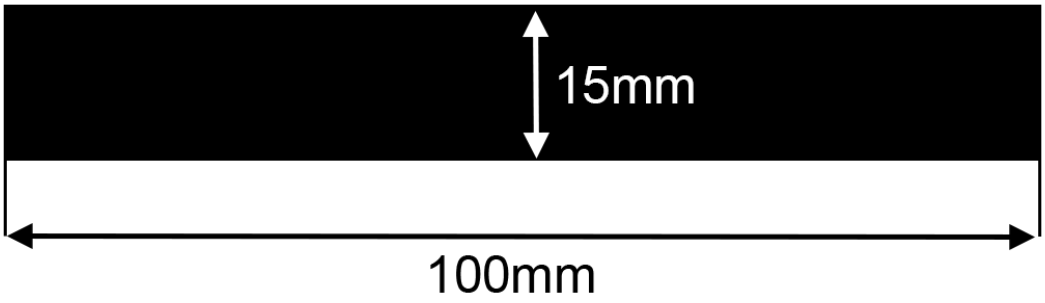

Figure 39 Dimensions of the strip test specimen

3.7 Tensile test description

In determining the elongation of the material in the machine to which a pull has been applied, it is necessary to perform tensile tests of all chosen films.

A tensile test is a fundamental materials science test where a sample is subjected to a controlled tension until failure. The properties that are directly measured include ultimate tensile strength, maximum elongation, and reduction in area. From these measurements, the following properties can also be determined: Young's modulus, Poisson's ratio, yield strength, and strain-hardening characteristics.

The test itself involves taking a standard-sized sample of the material with a fixed cross-sectional area, and then pulling it steadily with a tensimeter or a universal testing machine until it breaks. The machine has two grips that clamp the material; one grip remains stationary while the other moves to stretch the material. The tensile machine records the force applied to the specimen and the amount of elongation of the specimen over time. The force is measured in Newtons [N] and the elongation in millimeters [mm] while the stress is in the ratio of the Force and the cross-sectional area of the specimen and it's usually measured in Pascal [Pa].

3.8 Conditioning

Before conducting tensile tests, it is necessary for the samples to undergo conditioning to achieve the right temperature and relative humidity conditions of the material. With reference to the tests performed at room temperature, the specimens were stored for 40 hours in a room at $23 \pm 2°C$ with $50 \pm 10\%$ relative humidity and subsequently tested in a laboratory where the same temperature and humidity conditions were present. As for the hot tensile tests, the specimens were also stored before testing for 40 hours at $23 \pm 2°C$ with $50 \pm 10\%$ relative humidity, but once the temperature in the hot chamber was set and reached, the specimens were inserted into the grips and left to condition closed inside for 20 minutes so that they could reach thermal equilibrium with the hot chamber. It is important to condition the specimens well in order to have at least comparable test results because a higher relative humidity percentage has a plasticizing effect, thus negatively influencing the elastic moduli, and the same is true for a temperature difference [20] [22].

3.9 Test performed

The **first round** of tests was conducted in the laboratories of Politecnico di Milano at Via Mancinelli and consisted of hot tensile tests using dog bone-shaped specimens of

the dimensions indicated in the previous chapters. The machine's clamps featured a serrated surface for better grip on the specimen. The specimen conditioning was followed as mention in the chapter before, while the grip separation speeds were chosen to be 25 mm/min, as opposed to the recommended 2.5 mm/min specified in ASTM D882 – 10 standard. This was done to ensure the completion of all selected tests due to a fixed machine time allocation. Temperature tested were 30/60/80°C with a minimum of 3 specimens per test up to 5 when necessary. All tests were conducted for both the MD (Machine Direction) and TD (Transverse Direction) of the materials. Regarding all the "non-standard" conditions, a second round of tests will be conducted to verify that the chosen conditions did not influence the test results.

The **second round** of tensile tests was carried out at the company's facilities under ambient temperature conditions of 23±2°C and 50±10% relative humidity, using standard-sized specimens, which are strips long enough to ensure an initial grip separation of at least 100mm. It is important to note the change in the testing machine used for the second round of tensile tests, as well as the change in grips, which transitioned from serrated grips in the first round to flat grips in the second round. The specimens were tested both at the grip separation speed specified in ASTM D882-10 standard (10 mm/min) and at a speed of 25mm/min, as conducted in the first round of tests. An additional set of tensile tests at ambient temperature and 50% RH, but with a grip separation speed of 250mm/min, was performed for all specimens, including a single set at a speed of 1 mm/min specifically for the PEMDOTT specimen. Regarding the second round, all tests were done only for the MD (machine direction) due to time constriction. All tests were conducted using 3 specimens up to 5 when necessary.

All test conditions are summed in a table 4.2 and 4.3.

First round of tensile test using dog bone-shaped, after conditioning at 23±2°C and 50±10% RH for 40 hours and 20 minutes condition for reaching equilibrium with the hot chamber:

Table 3.3 Summary of hot tensile test parameters for the first round of testing

	pemdott	EXC21008	EXC22004	EX23453	EX21011	mopott
T 23°C						
T 30°C	X	X	X	X	X	X
T 60°C	X	X	X	X	X	X
T 80°C	X	X	X	X	X	X
N °of specimens	3-5	3-5	3-5	3-5	3-5	3-5
MD	X	X	X	X	X	X
TD	X	X	X	X	X	X
$v_{grip\ separation}\ 1\frac{mm}{min}$						
$v_{grip\ separation}\ 10\frac{mm}{min}$						
$v_{grip\ separation}\ 25\frac{mm}{min}$	X	X	X	X	X	X
$v_{grip\ separation}\ 250\frac{mm}{min}$						

First round of tensile test strips with an initial grip separation of 100mm, after conditioning at 23±2°C and 50±10% RH for 40 hours and kept at room temperature:

Table 3.4 Summary of hot tensile test parameters for the second round of testing

	pemdott	EXC21008	EXC22004	EX23453	EX21011	mopott
T 23°C	X	X	X	X	X	X
T 30°C						
T 60°C						
T 80°C						
N °of specimens	3-5	3-5	3-5	3-5	3-5	3-5
MD	X	X	X	X	X	X
TD						
$v_{grip\ separation}\ 1\frac{mm}{min}$	X					
$v_{grip\ separation}\ 10\frac{mm}{min}$	X	X	X	X	X	X
$v_{grip\ separation}\ 25\frac{mm}{min}$	X	X	X	X	X	X
$vv_{grip\ sepaation}\ 250\frac{mm}{min}$	X	X	X	X	X	X

For all the tested specimens in both rounds, the thickness of each specimen was measured using a micrometer, and the width of the usable section was measured using callipers. The data sampling frequency was set on the machine at 10Hz.

3.10 Data processing and cleaning

After conducting the tensile tests, the machinery generates a text file containing the load [N] and the specimen extension [mm]. The files were imported into Microsoft

Excel® and automatically divided into columns; all data processing was carried out using Excel®. An initial data cleaning was necessary because, before recording applied load values on the specimen, the machinery must tension it and ensure precise positioning. In the data, there may be a "moment of uncertainty" in the machinery with values oscillating around 0 N of load (including recording negative loads). Once the machinery reaches 0.05N of load, the tensile test actually begins, so it was necessary to remove all data preceding the 0.05N load value and ensure that the specimen's extension value is reset to the first valid load value. Data cleaning was also performed regarding material failure, with the elimination of all data immediately following the collapse to 0 N load on the specimen after fracture.

It is also important to eliminate data from all specimens whose fracture did not occur within the usable section but near the grips, or from specimens whose premature rupture may suggest the presence of tears on the specimen's edge. In figure 41, you can see some examples of discarded specimens and retained specimens.

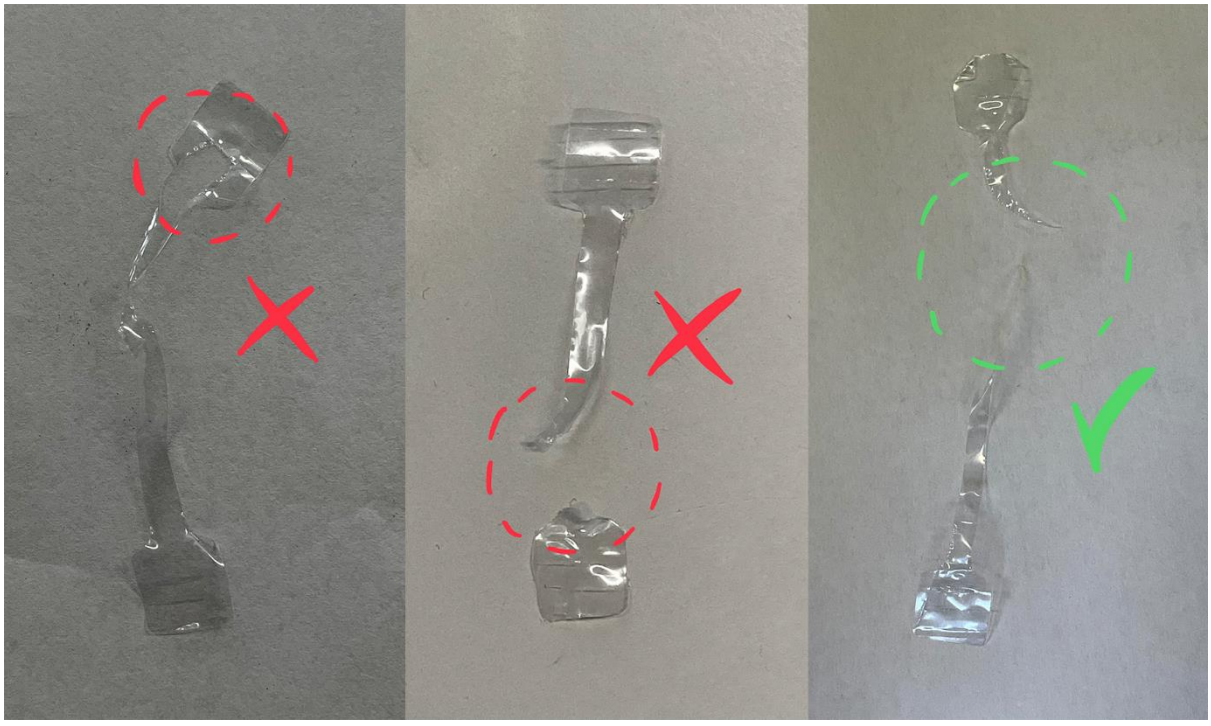

Figure 40 example of discarded specimens on the left and center while an example of retained specimens on the right

Subsequently, the cross-sectional area of the specimen is calculated, having measured the thickness and width of the usable section before placing it in the machine. The calculated area was then used to obtain the strain data according to the formula 3.1

$$\sigma = \frac{F}{A_{cross-sectional}} \tag{3.1}$$

Where:

- F is the load [N] applied by the machine
- $A_{cross-sectional}$ $[m^2]$ is the product of thickness and width of usable section
- σ [Pa] is the stress applied

The strain ε was calculated as explained in equation 2.4 and the multiplied by 100 to obtain the strain %. Once all stress points and their corresponding strain % values were calculated, the data was plotted to obtain a stress-strain curve. In some cases where the stress-strain curve graphs appeared to be very noisy, it was necessary to apply data smoothing using a 5-sample moving average while maintaining the starting and ending points of the curve at 0 Mpa for the stress value. In cases where this technique was applied, it will be indicated.

The calculation of Young's modulus was performed by applying linear regression to the initial points of the stress-strain curve, where a linear trend of the curve should be observed as it is in the elastic region, using the tool available in the creation of scatterplots in Microsoft Excel®. Only linear regressions with an R-squared value exceeding 0.9 were accepted.

Since the company's focus is on the elastic modulus values from the curves, data processing was carried out exclusively for the elastic modulus in both the machine direction and transverse direction. The elastic modulus data was used to find an average value for each temperature, as well as the corresponding sample standard deviation, for both the first and second rounds, in order to understand the consistency of the collected data.

The data from the first round of tensile tests at 30, 60, and 80°C were used to develop a model that could establish a relationship between Young's modulus and the material's operating temperature. After a phase of data snooping and a literature search, it was chosen to interpolate the data using an exponential model [23]. The found model was then put to the test by validating it with the second round of data collected at room temperature (taking into account variations due to the change in machine and grips). All the considerations regarding the specimen fractures made for the first round of tests were also applied to the second round, with the only difference being the use of a strip of dimensions as expressed in the previous chapter

4 Results

This section will present the results of the tensile tests for all materials, starting with the outcomes from the first round of testing, which involved "dog-bone" shaped specimens at temperatures of 30, 60, and 80°C. The results will first showcase the entire stress-strain curve of all the suitable specimens tested at the temperatures chosen. A focus will then be placed on the curves in the initial stretch of elongation, specifically up to a deformation of 10%. This is particularly useful for understanding and comparing the curves at different temperatures, as the initial elastic part of the curve would appear very "flattened" in cases of very high elongation at break, obscuring the thesis's objective. Subsequently, Young's modulus and relative standard deviation values derived for each acceptable specimen will be presented. As mentioned in the previous chapter, only results of linear interpolations with an R^2 value greater than 0.9 were considered, reflecting the theoretically linear behavior in the elastic region. Given the thesis's focus on materials used in the converting phase, properties in the machine direction (MD) are more significant than those in the transverse direction (TD). Additionally, a comparison of various materials will be made to clarify which ones have the best mechanical properties under identical operating conditions. **In the next chapter,** the data presented will be use to formulate an exponential model in order to correlate Young's modulus with the operating temperature. These models will be compared and validated using data from the second round of tensile tests performed in the company at room temperature following standard conditions. This will also help confirm that the use of non-standard sizes and speeds in the first round did not influence the test results. For the second round, only the values of the Young's moduli obtained and the corresponding standard deviation will be presented.

4.1 Tensile test results

The results of tensile tests conducted at different grip separation speeds will be presented. The purpose of this is to understand if there is a correlation between the grip separation speed and the recorded Young's modulus. By exploring this aspect, the study aims to determine whether the speed at which the material is stretched impacts its elastic properties, as measured by Young's modulus.

4.1.1 PEMDOTT machine direction

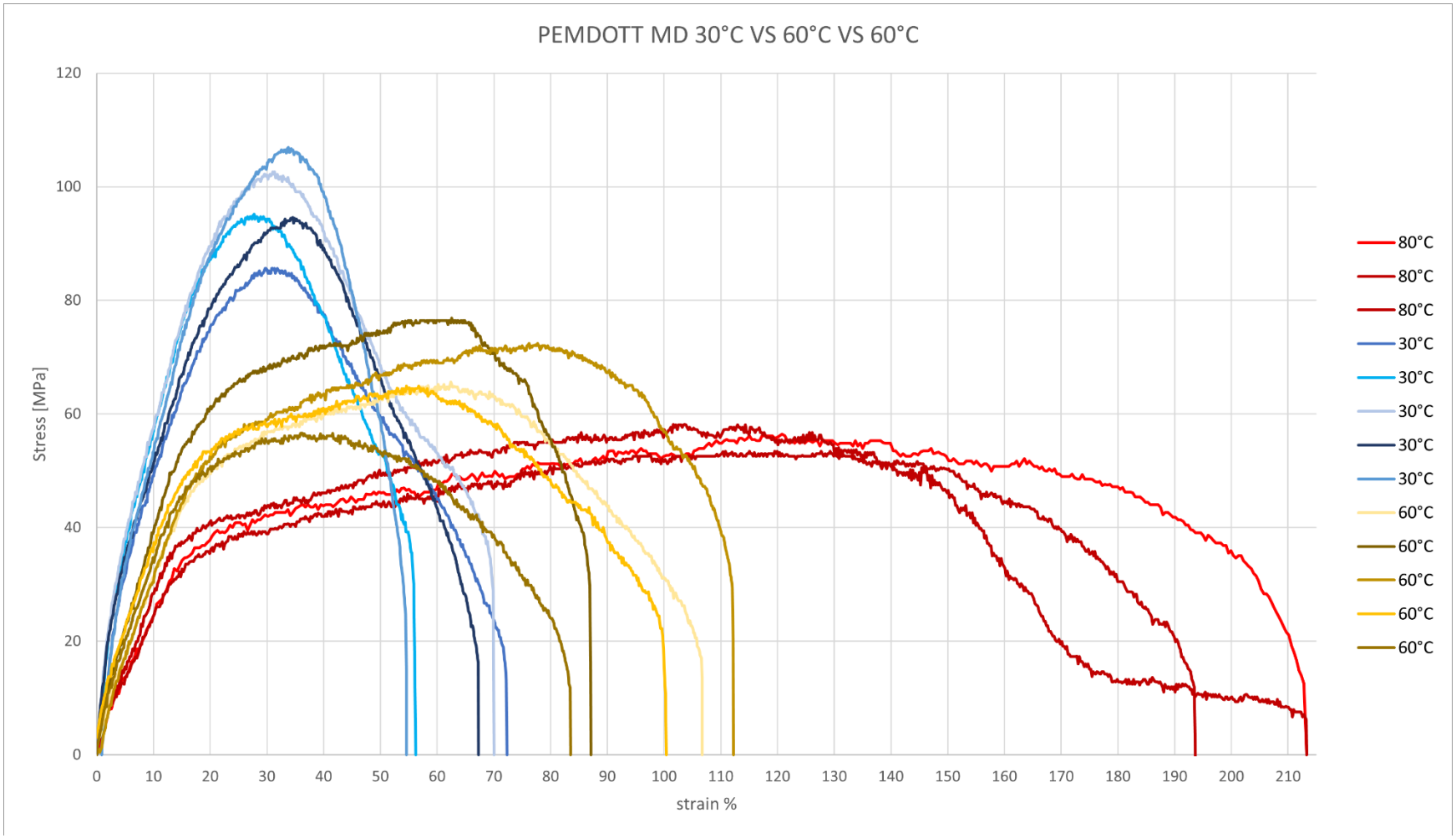

Figure 32 Stress-strain curve for PEMDOTT machine direction of specimens tested at 30°C (blue), 60°C (yellow), 80°C (red)

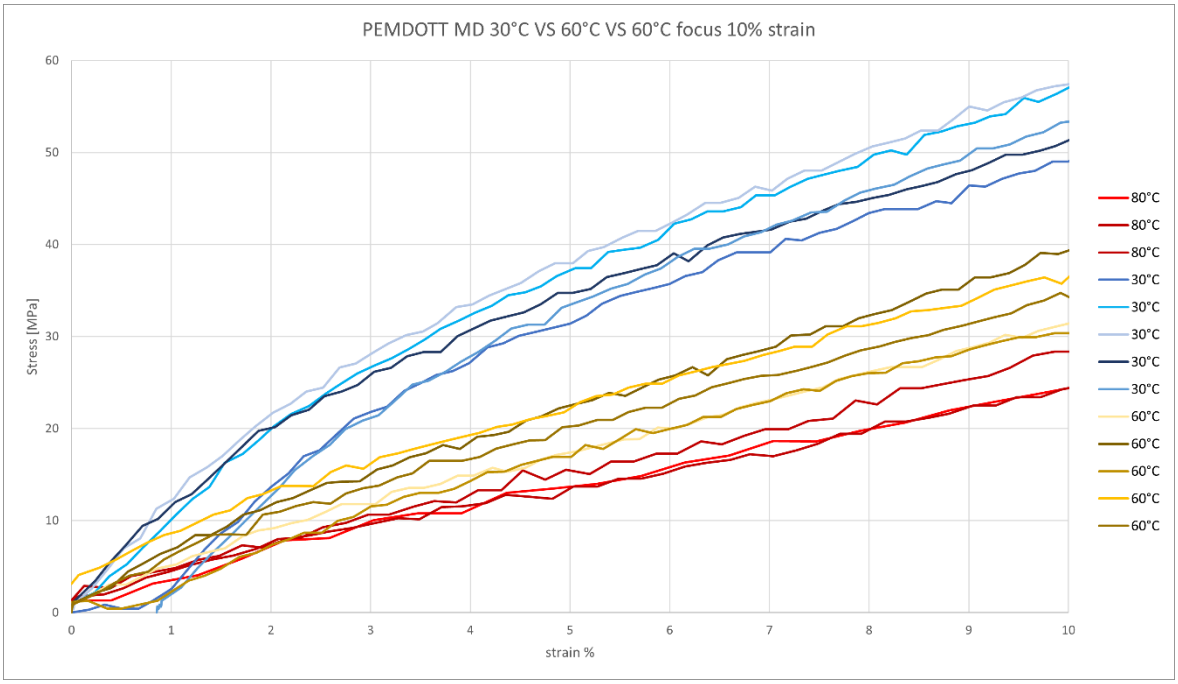

Figure 33 Stress-strain curve focus strain up to 10% for PEMDOTT machine direction of specimens tested at 30°C (blue), 60°C (yellow), 80°C (red)

Table 4.1 Young's modulus from linear regression on stress-strain curve for 30,60 and 80°C

Young's Modulus tested specimens PEMDOTT MD												
30°C					60°C					80°C		
880.9	970.1	970.9	825.9	927.8	297.3	396.6	317.4	349.2	345.4	226.1	205.3	256.8
average	915.1	MPa			average	341.1	MPa			average	229.4	MPa
st	62.1	MPa			st	37.6	MPa			st	25.9	MPa

The data presented in table 4.1 indicates a significant decrease in the elastic modulus with increasing temperature. More specifically, there is a 63% decrease in the modulus of elasticity when the temperature rises from 30°C to 60°C, followed by a further 33% reduction in the Young's modulus from 60°C to 80°C. Overall, this amounts to a substantial 75% decrease in the Young's modulus when the temperature range shifts from 30°C to 80°C.

These results are indicative of a notable sensitivity of the material's elastic properties to temperature changes. The sharp decline in the elastic modulus with increasing temperature suggests that the material deforms with a lesser force for the same level of elongation.

4.1.2 EXC21011 machine direction

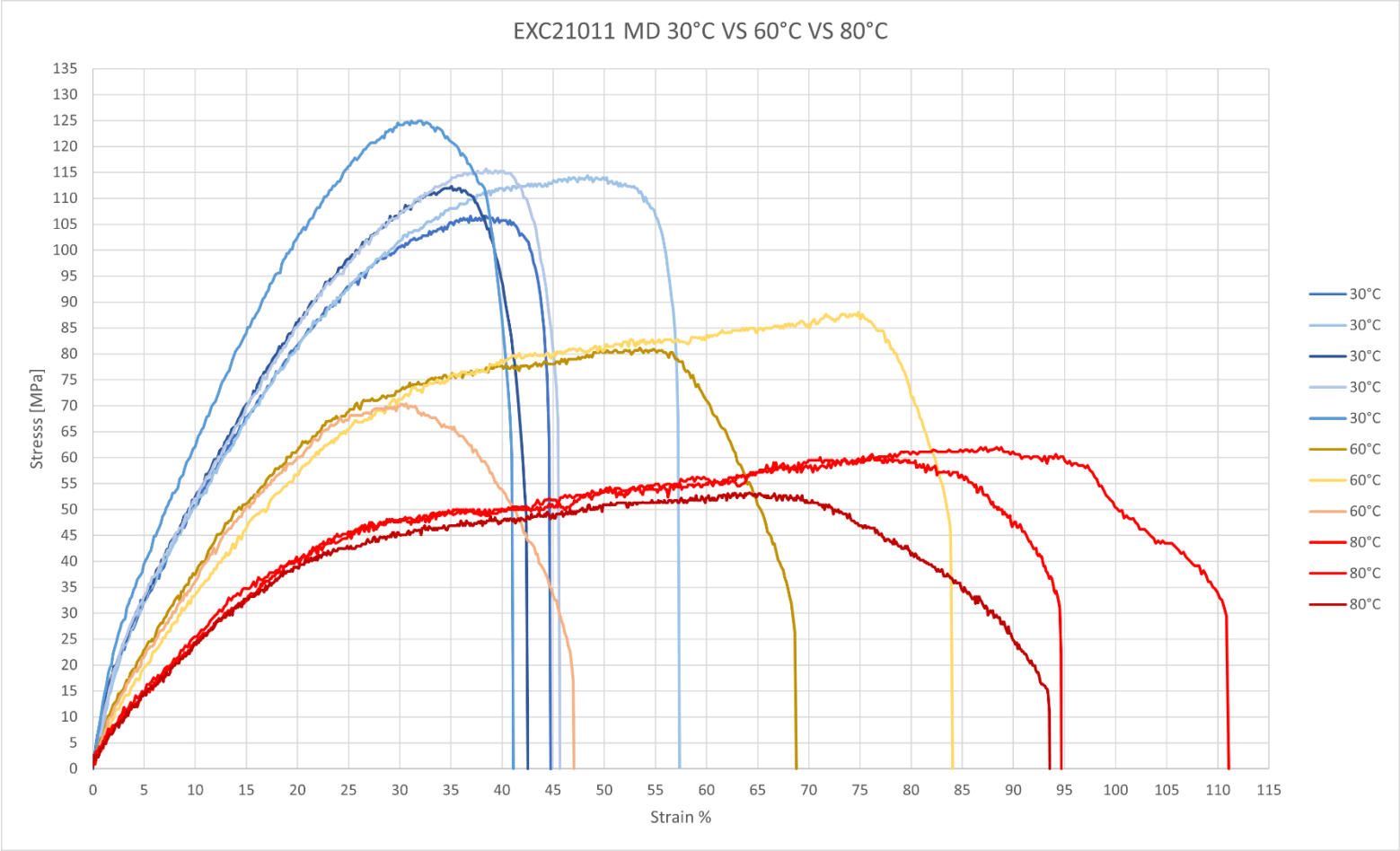

Figure 34 Stress-strain curve for EXC21011 machine direction of specimens tested at 30°C (blue), 60°C (yellow), 80°C (red)

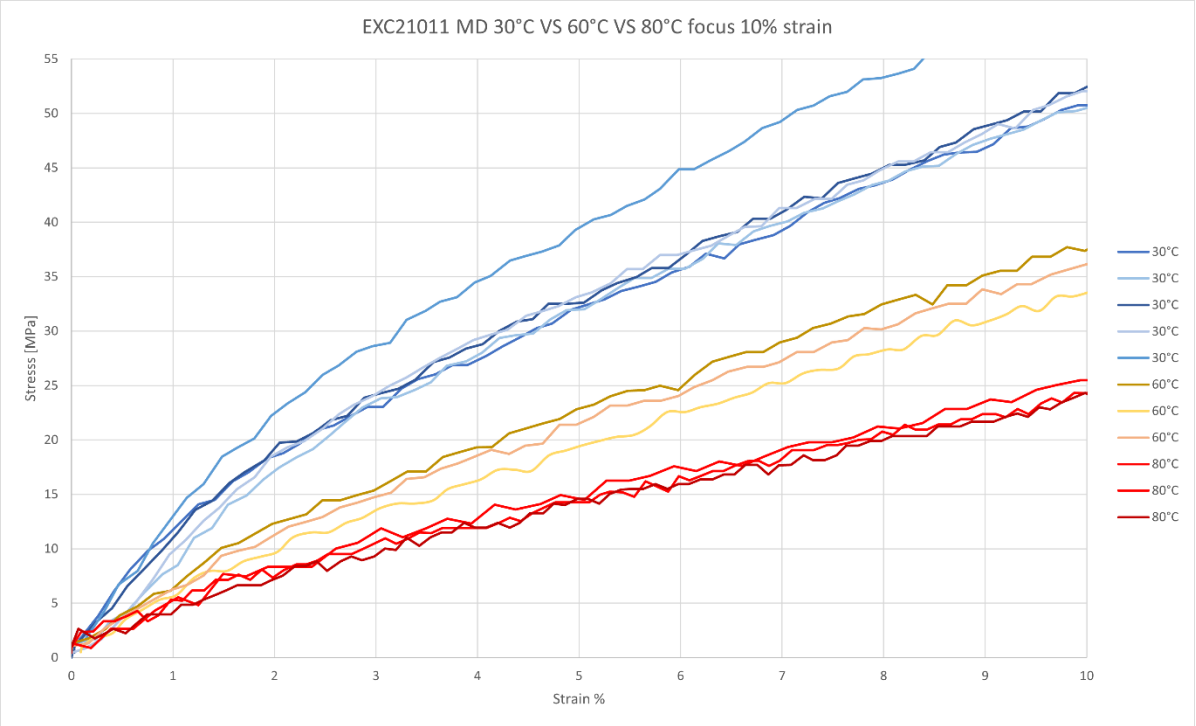

Figure 35 Stress-strain curve focus strain up to 10% for EXC21011 machine direction of specimens tested at 30°C (blue), 60°C (yellow), 80°C (red)

Table 4.2 Young's modulus from linear regression on stress-strain curve for 30,60 and 80°C

Young's Modulus tested specimens EXC21011 MD										
30°C					60°C			80°C		
1026.2	843.7	1048.2	992.8	1213.2	483.3	399.0	446.4	218.9	228.4	226.9
average	1024.8	MPa			average	442.9	MPa	average	224.7	MPa
st	132.2	MPa			st	42.3	MPa	st	5.1	MPa

The data presented in table 4.2 indicates a significant decrease in the elastic modulus with increasing temperature. More specifically, there is a 57% decrease in the modulus of elasticity when the temperature rises from 30°C to 60°C, followed by a further 49% reduction in the Young's modulus from 60°C to 80°C. Overall, this amounts to a substantial 78% decrease in Young's modulus when the temperature range shifts from 30°C to 80°C.

These results are indicative of a notable sensitivity of the material's elastic properties to temperature changes. The sharp decline in the elastic modulus with increasing temperature suggests that the material deforms with a lesser force for the same level of elongation.

4.1.3 EXC23453 machine direction

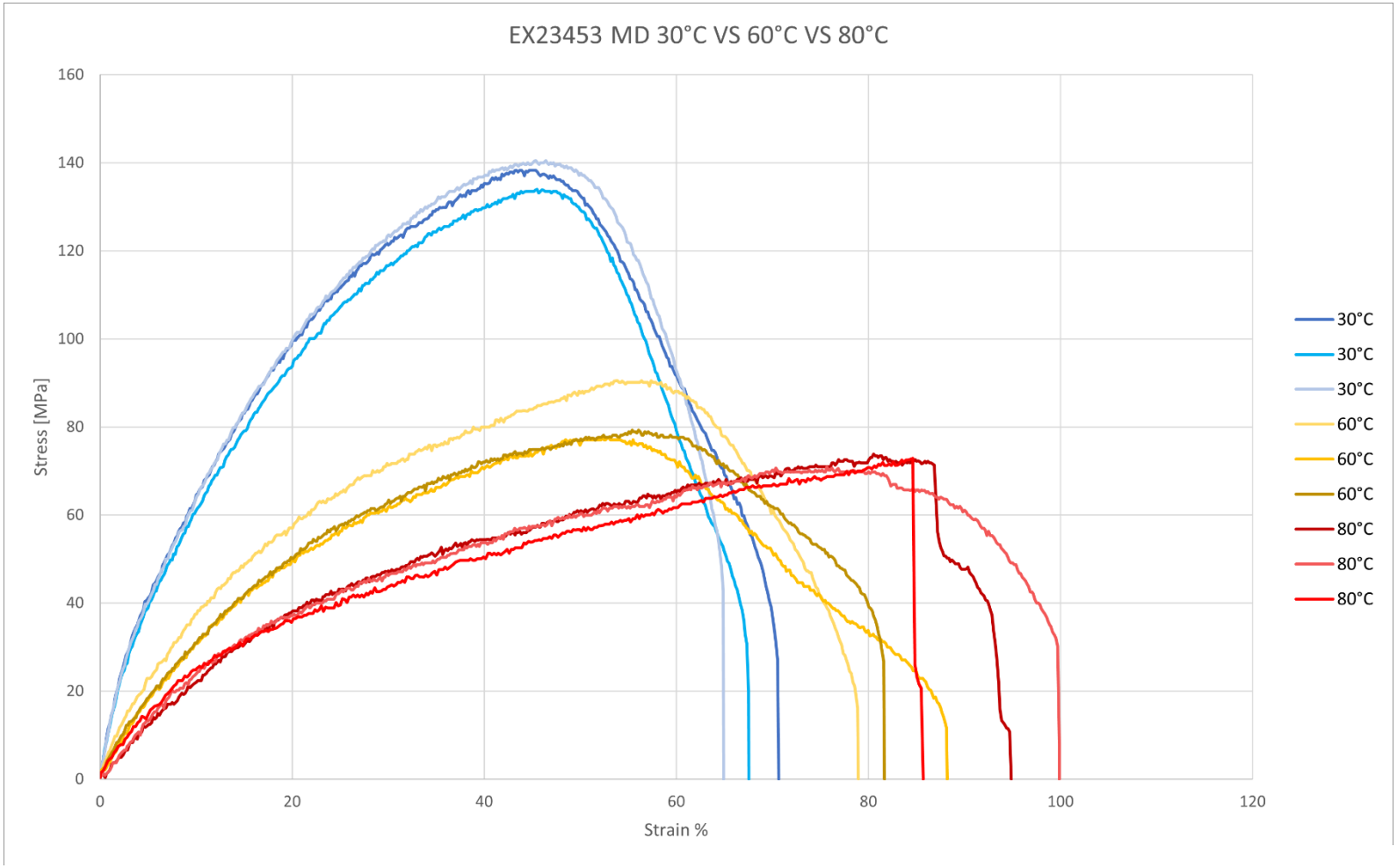

Figure 36 Stress-strain curve for EX23453 machine direction of specimens tested at 30°C (blue), 60°C (yellow), 80°C (red)

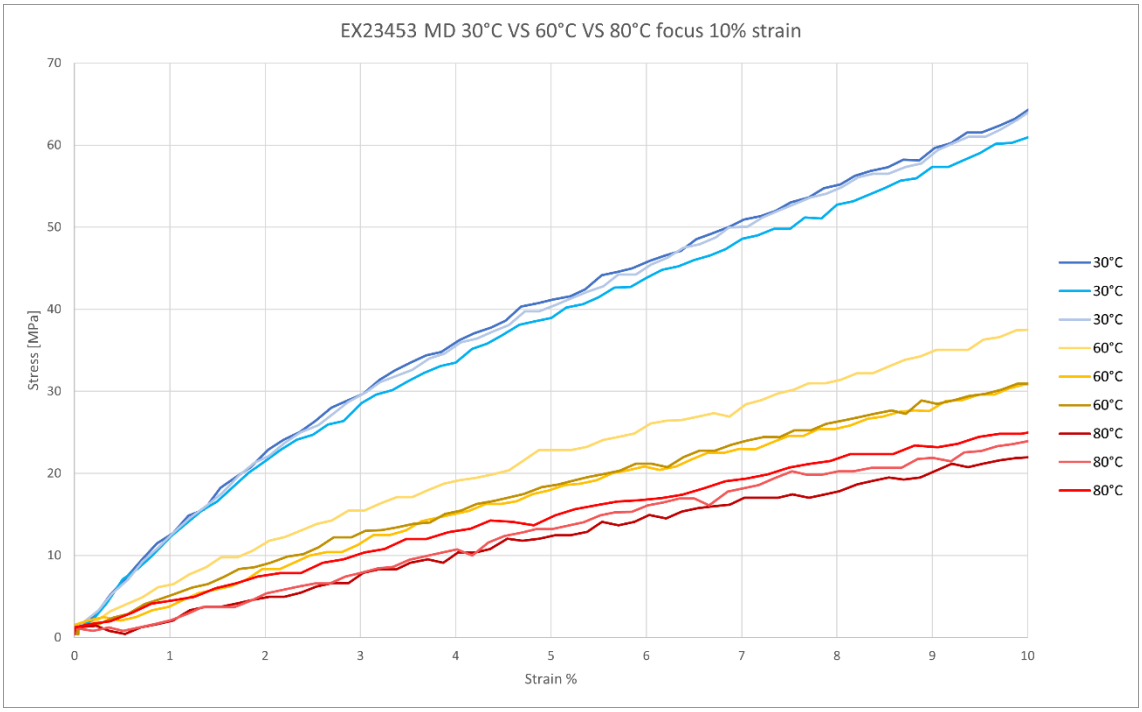

Figure 37 Stress-strain curve focus strain up to 10% for EX23453 machine direction of specimens tested at 30°C (blue), 60°C (yellow), 80°C (red)

Table 4.3 Young's modulus from linear regression on stress-strain curve for 30,60 and 80°C

Young's Modulus tested specimens EX23453 MD								
30°C			60°C			80°C		
1059.7	1006.5	1047.1	480.6	366.7	366.4	250.5	279.4	286.5
average	1037.8	MPa	average	404.6	MPa	average	272.1	MPa
st	27.8	MPa	st	65.8	MPa	st	19.1	MPa

The data presented in table 4.3 indicates a significant decrease in the elastic modulus with increasing temperature. More specifically, there is a 60% decrease in the modulus of elasticity when the temperature rises from 30°C to 60°C, followed by a further 33% reduction in the Young's modulus from 60°C to 80°C. Overall, this amounts to a substantial 74% decrease in Young's modulus when the temperature range shifts from 30°C to 80°C.

These results are indicative of a notable sensitivity of the material's elastic properties to temperature changes. The sharp decline in the elastic modulus with increasing temperature suggests that the material deforms with a lesser force for the same level of elongation.

4.1.4 EXC22004 machine direction

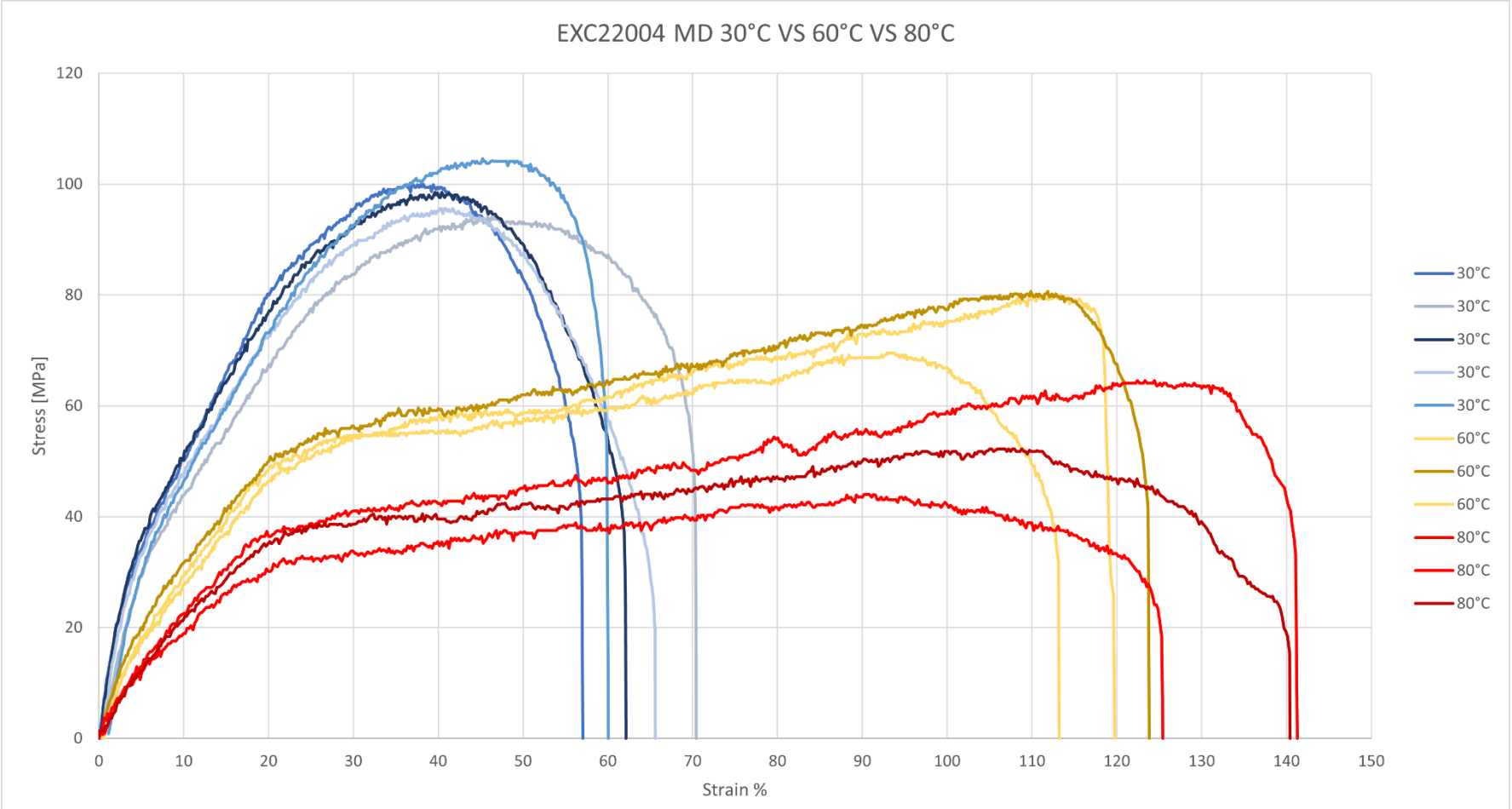

Figure 38 Stress-strain curve for EXC22004 machine direction of specimens tested at 30°C (blue), 60°C (yellow), 80°C (red)

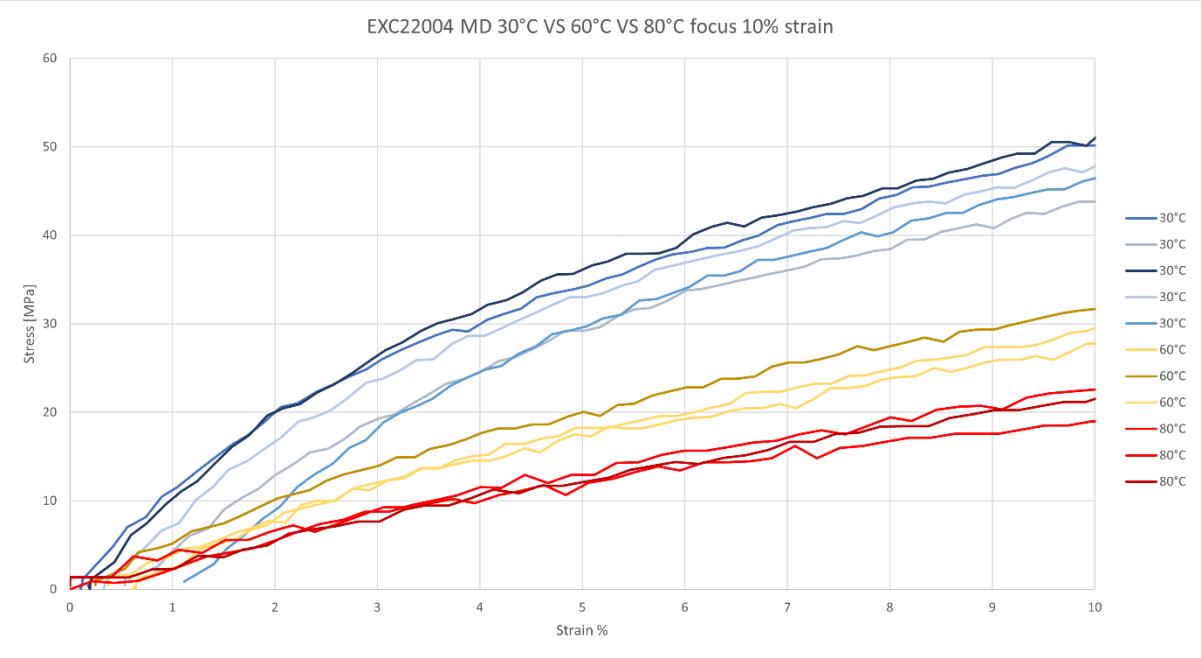

Figure 39 Stress-strain curve focus strain up to 10% for EXC22004 machine direction of specimens tested at 30°C (blue), 60°C (yellow), 80°C (red)

Table 4.4 Young's modulus from linear regression on stress-strain curve for 30,60 and 80°C

Young's Modulus tested specimens EXC22004 MD										
30°C					60°C			80°C		
1081.5	772.1	843.7	1054.6	929.5	426.8	378.5	343.2	273.9	196.6	234.8
average	936.2	MPa			average	382.8	MPa	average	235.1	MPa
St	132.9	MPa			st	41.9	MPa	st	38.6	MPa

The data presented in table 4.4 indicates a significant decrease in the elastic modulus with increasing temperature. More specifically, there is a 60% decrease in the modulus of elasticity when the temperature rises from 30°C to 60°C, followed by a further 39% reduction in the Young's modulus from 60°C to 80°C. Overall, this amounts to a substantial 75% decrease in Young's modulus when the temperature range shifts from 30°C to 80°C.

These results are indicative of a notable sensitivity of the material's elastic properties to temperature changes. The sharp decline in the elastic modulus with increasing temperature suggests that the material deforms with a lesser force for the same level of elongation.

4.1.5 EXC21008 machine direction

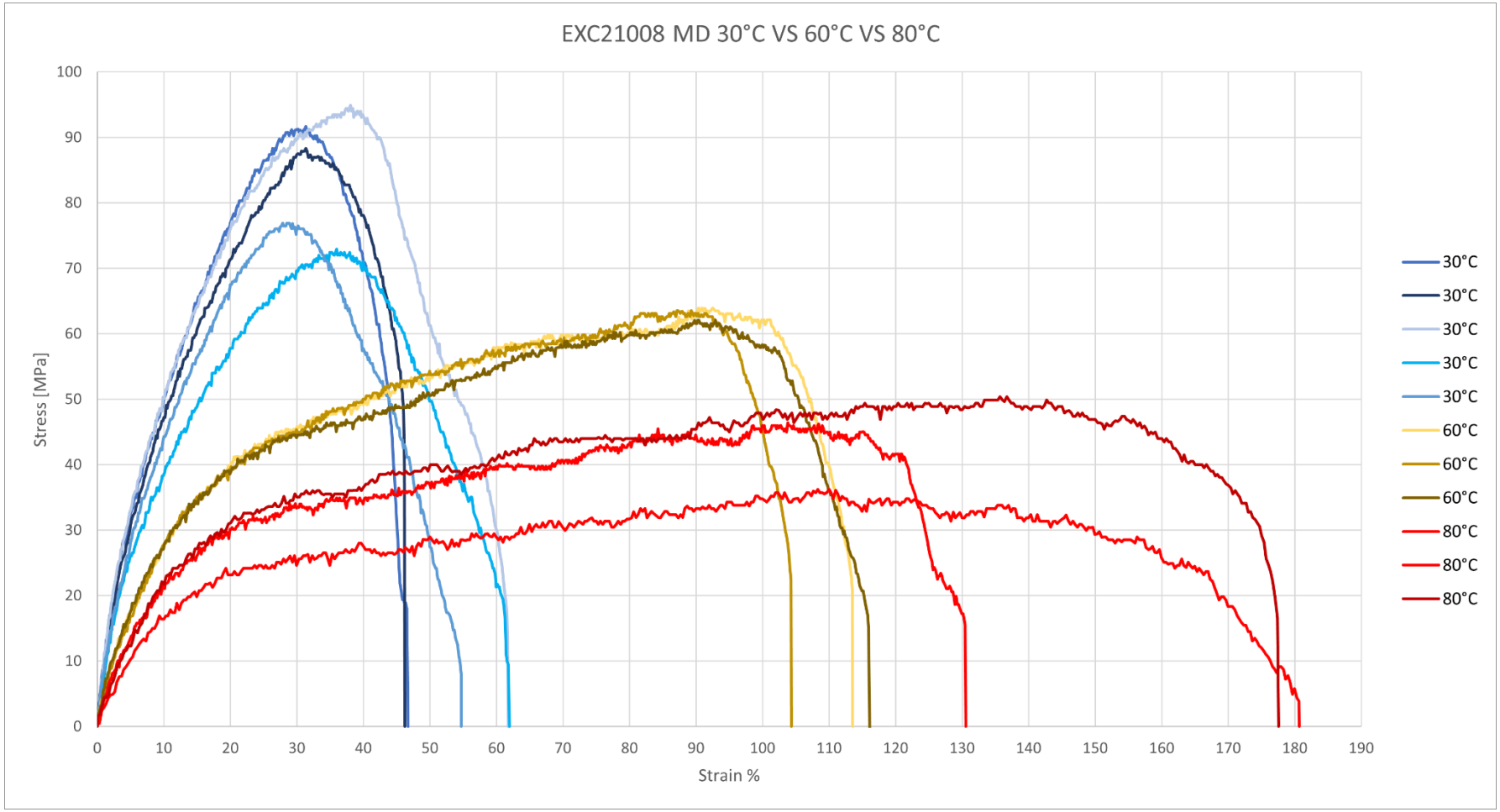

Figure 40 Stress-strain curve for EXC21008 machine direction of specimens tested at 30°C (blue), 60°C (yellow), 80°C (red)

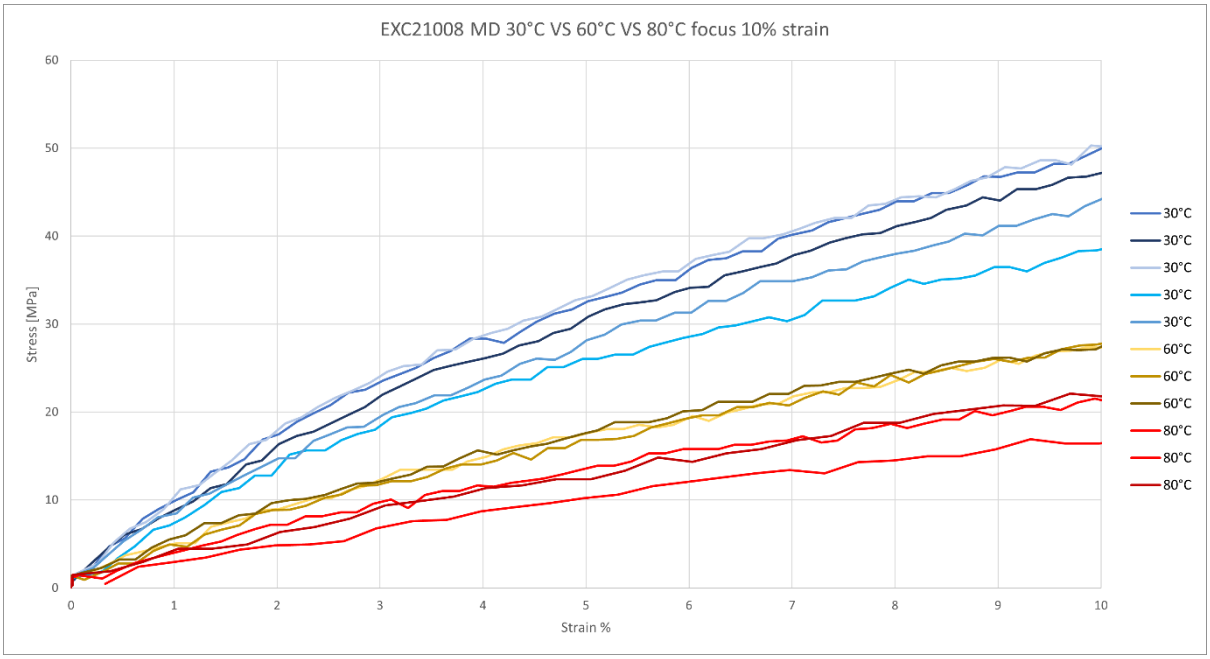

Figure 41 Stress-strain curve focus strain up to 10% for EXC21008 machine direction of specimens tested at 30°C (blue), 60°C (yellow), 80°C (red)

Table 4.5 Young's modulus from linear regression on stress-strain curve for 30,60 and 80°C

Young's Modulus tested specimens EXC21008 MD										
30°C					60°C			80°C		
847.7	704.0	874.4	673.9	699.5	334.5	325.6	329.0	174.6	280.7	231.1
average	759.9	MPa			average	329.7	MPa	average	228.8	MPa
st	93.5	MPa			st	4.5	MPa	st	53.1	MPa

The data presented in table 4.5 indicates a significant decrease in the elastic modulus with increasing temperature. More specifically, there is a 57% decrease in the modulus of elasticity when the temperature rises from 30°C to 60°C, followed by a further 30% reduction in the Young's modulus from 60°C to 80°C. Overall, this amounts to a substantial 70% decrease in Young's modulus when the temperature range shifts from 30°C to 80°C.

These results are indicative of a notable sensitivity of the material's elastic properties to temperature changes. The sharp decline in the elastic modulus with increasing temperature suggests that the material deforms with a lesser force for the same level of elongation

4.1.6 MOPOTT machine direction

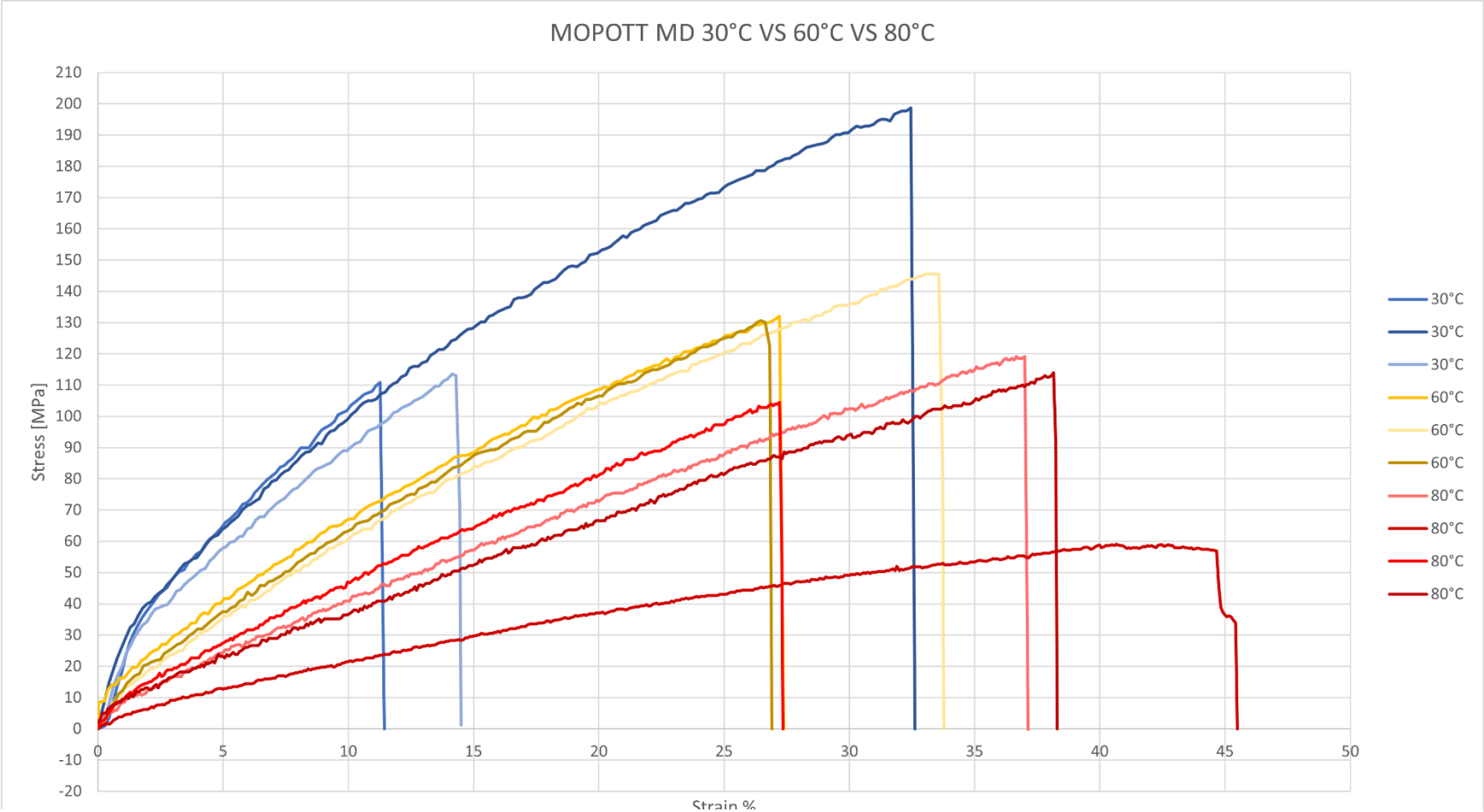

Figure 42 Stress-strain curve for MOPOTT machine direction of specimens tested at 30°C (blue), 60°C (yellow), 80°C (red)

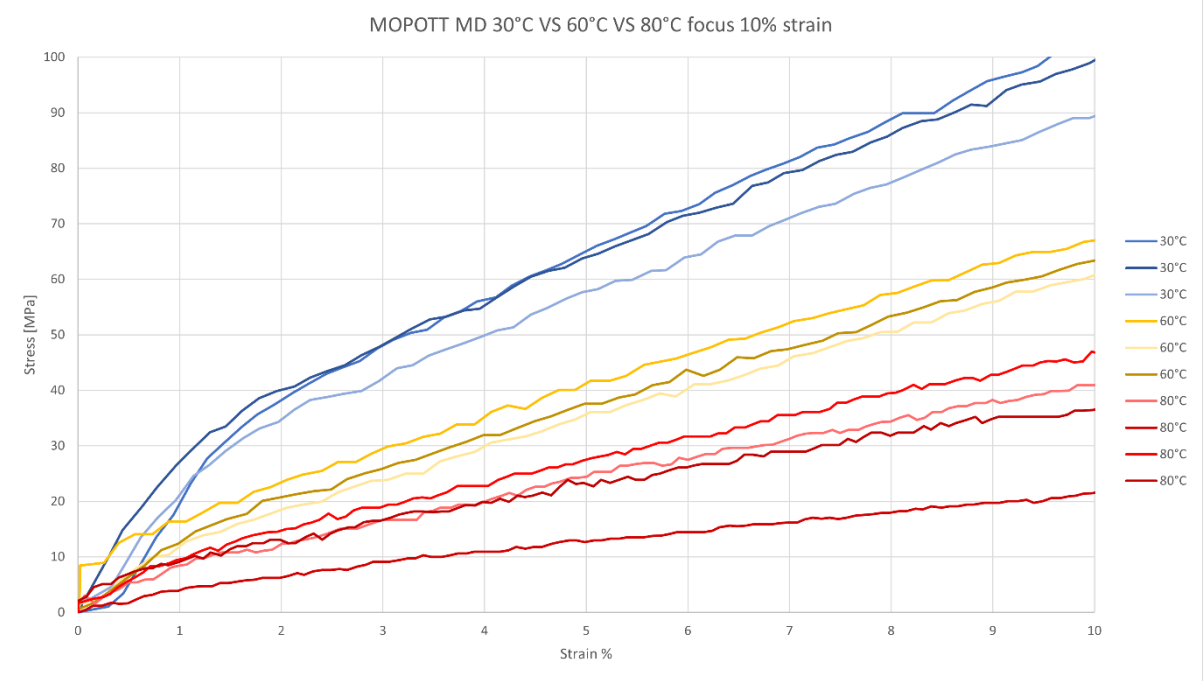

Figure 43 Stress-strain curve focus strain up to 10% for MOPOTT machine direction of specimens tested at 30°C (blue), 60°C (yellow), 80°C (red)

Table 4.6 Young's modulus from linear regression on stress-strain curve for 30,60 and 80°C

Young's Modulus tested specimens MOPOTT MD								
30°C			60°C			80°C		
1°	2°	3°	1°	2°	3°	1°	2°	3°
2784.5	3057.3	2266.6	969.9	841.5	1137.8	701.2	861.8	544.9
average	2702.8	MPa	average	983.0	MPa	average	702.6	MPa
st	401.6	MPa	st	148.6	MPa	st	158.4	MPa

The data presented in table 4.6 indicates a significant decrease in the elastic modulus with increasing temperature. More specifically, there is a 64% decrease in the modulus of elasticity when the temperature rises from 30°C to 60°C, followed by a further 29% reduction in the Young's modulus from 60°C to 80°C. Overall, this amounts to a substantial 75% decrease in Young's modulus when the temperature range shifts from 30°C to 80°C. These results are indicative of a notable sensitivity of the material's elastic properties to temperature changes. The sharp decline in the elastic modulus with increasing temperature suggests that the material deforms with a lesser force for the same level of elongation.

4.2 Comparison of the results

4.2.1 Comparison between material tested

In this section, we present a summary of all the average values of Young's modulus along with their respective standard deviations for all the tested materials, grouped according to operating conditions. For a fairer comparison among MDO PE materials, the first graph considers only MDO PE, while in the second graph, BOPP (MOPOTT) is also included.

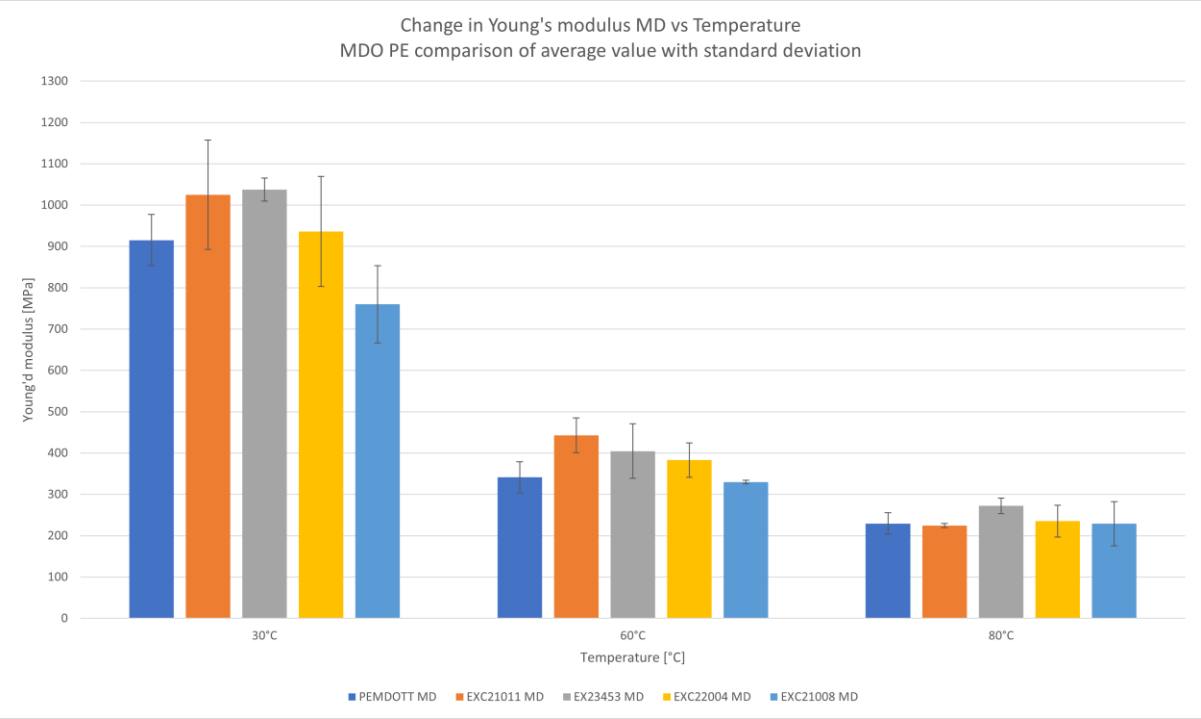

Figure 44 Comparison between Young's modulus and their respective standard deviation for only MDO PE specimens in MD

From the analysis of figure 53, it's evident that the disparity in the Young's modulus values of different materials becomes less pronounced with an increase in the operating temperature.

In terms of specific materials, there are notable differences in performance. For example, the MDO PE material labelled as EXC21008 consistently shows inferior properties compared to its counterparts across the range of temperatures tested. This could indicate a fundamental difference in the composition or manufacturing process of EXC21008, leading to its lower performance.

On the other hand, when focusing on the tests conducted at 60°C, which align closely with real-world operating conditions, EXC21011 emerges as the better MDO PE material, demonstrating the highest Young's modulus. This is closely followed by EX23453 and EXC22004. The high performance of EXC21011 could be attributed to its material composition, processing methods, or other factors that contribute to its enhanced elastic properties.

Interestingly, these observations and rankings of material performance are consistent even at the higher temperature test of 80°C. This consistency across different temperatures further validates the relative performance of these materials under varying thermal conditions.

Such findings are critical for material selection in applications where temperature plays a significant role in material behaviour. Choosing the right material, such as EXC21011 for applications that demand high modulus at elevated temperatures, can significantly impact the product's functionality and durability.

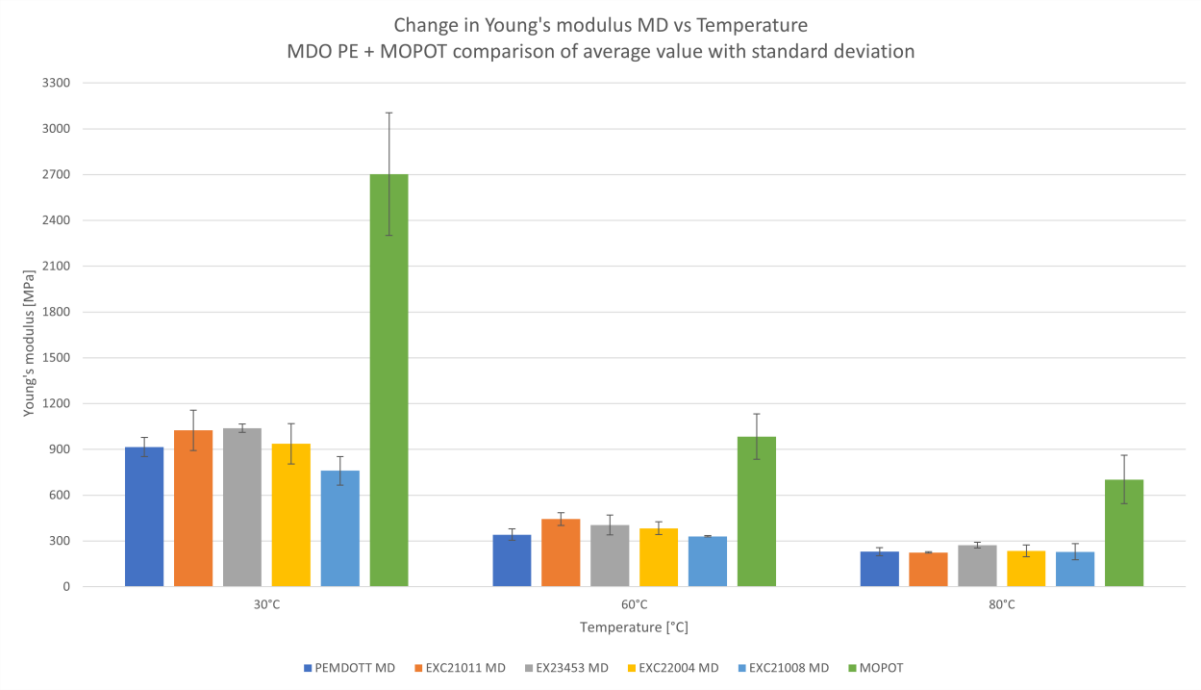

Figure 45 Comparison between Young's modulus and their respective standard deviation for MDO PE and BOPP specimens in MD

From figure 54, it is noticeable that MOPOTT, the only material in the tests made of BOPP, exhibits significantly superior performance compared to all other MDO PE materials across all temperature conditions. The Young's moduli of MOPOTT are distinctly higher, about 2-3 times greater than those of the other materials, making MOPOTT the best material in terms of resistance to elastic deformation.

Moreover, the consistency of MOPOTT's superior performance across different temperatures further solidifies its suitability for applications with varying thermal environments. Its ability to maintain high levels of resistance to deformation, even at elevated temperatures, is a valuable characteristic in many industrial and commercial applications.

Table 4.7 Drop in Young's Modulus of all material tested in different temperature conditions

	pemdott MD	**exc21011 MD**	**ex23453 MD**	**exc22004 MD**	**exc21008 MD**	**mopott MD**
from 30°C to 60°C	- 63%	- 57%	- 60%	- 60%	- 57%	- 64%
from 60°C to 80°C	- 33%	- 49%	- 33%	- 39%	- 30%	- 29%
Overall from 30°C to 80°C	- 75%	- 78%	- 74%	- 75%	- 70%	- 75%

The table 4.7 summarizes the percentage drops in Young's modulus across varying operating conditions. It is noticeable that the variations are quite similar for all MDO PE materials, especially the final change from 30°C to 80°C, which is close to -74% for all materials. This result could be anticipated, considering the comparison is among very similar materials. However, this trend is also confirmed by MOPOTT, a BOPP material, which also exhibits a change in Young's modulus from 30°C to 80°C of -75%, despite not being an MDO PE. These results could indicate that the change in Young's modulus due to temperature variation might be similar even among plastic materials not belonging to the same family, like MDO PE and BOPP. However, it's important to note that this trend, while suggestive, is not conclusive evidence of a universal thermal response in all plastics. The fact that these materials show similar trends does raise interesting questions about the thermal behaviour of different plastic families, but it also highlights the need for further research. Specifically, it would be valuable to investigate whether this trend holds true for a wider range of plastic materials and under different environmental conditions.

Such research could have significant implications for material science, particularly in understanding and predicting the behavior of plastics under thermal stress.

4.2.2 Comparison of results with literature and suppliers

By comparing the Young's modulus results with the data provided by the suppliers (table 3.1), it can be observed that the values found from the hot tests are generally smaller. This discrepancy is clearly due to the higher temperature values used to perform the tests. The Young's modulus values, in the case of MDO film, are also influenced by the draw ratio (DR), drawing speed, drawing temperature, and heat-setting conditions. In the literature, it is possible to find values around 2000 MPa [24] for the elastic modulus, a figure absolutely in line with the technical sheets of the materials sent by the suppliers and reasonably higher than the experimental data obtained, having been recorded under slightly different operating conditions.

4.3 Result for transverse direction

In table 4.8 to 4.13 are all the values obtained for the Young's modulus of all the specimens with respect to the transverse direction (TD).

Table 4.8 Young's modulus from linear regression on stress-strain curve for 30,60 and 80°C

Young's Modulus tested specimens PEMDOTT TD												
30°C					60°C					80°C		
493	438	524	777	621	436	602	484	528	502	520	435	407
average	571	MPa			average	511	MPa			average	454	MPa
st	133	MPa			st	61	MPa			st	59	MPa

Table 4.9 Young's modulus from linear regression on stress-strain curve for 30.60 and 80°C

Young's Modulus tested specimens EXC21011 TD										
30°C					60°C			80°C		
1102.4	742.1	808.3	774.1	975.3	505.1	502.6	352.6	367.6	349.1	325.6
average	880.4	MPa			average	453.4	MPa	average	347.4	MPa
st	153.2	MPa			st	87.3	MPa	st	21.0	MPa

Table 4.10 Young's modulus from linear regression on stress-strain curve for 30.60 and 80°C

Young's Modulus tested specimens EX23453 TD									
30°C			60°C				80°C		
631.8	780.8	766.3	391.7	432.6	432.9	479.8	292.8	249.1	415.2
average	726.3	MPa	average	434.2	MPa		average	319.0	MPa
st	82.2	MPa	st	36.0	MPa		st	86.1	MPa

Table 4.11 Young's modulus from linear regression on stress-strain curve for 30,60 and 80°C

Young's Modulus tested specimens EXC22004 TD								
30°C			60°C			80°C		
1014.9	692.4	1083.7	596.8	575.6	571.8	364.9	520.8	392.1
average	930.3	MPa	average	581.4	MPa	average	425.9	MPa
st	208.9	MPa	st	13.5	MPa	st	83.3	MPa

Table 4.12 Young's modulus from linear regression on stress-strain curve for 30.60 and 80°C

Young's Modulus tested specimens EXC21008 TD										
30°C				60°C				80°C		
416.0	226.2	484.3	341.6	207.3	176.2	175.2	196.7	193.4	233.9	396.1
average	367.0	MPa		average	188.8	MPa		average	274.5	MPa
st	110.5	MPa		st	15.8	MPa		st	107.2	MPa

Table 4.13 Young's modulus from linear regression on stress-strain curve for 30.60 and 80°C

Young's Modulus tested specimens MOPOTT TD								
30°C			60°C			80°C		
1607.0	1330.6	831.3	372.8	474.9	549.0	374.9	412.3	439.3
average	1256.3	MPa	average	465.5	MPa	average	408.8	MPa
st	393.2	MPa	st	88.5	MPa	st	32.4	MPa

In figure 55, we can better visualize the information obtained from the tensile tests. The different Young's moduli and their respective standard deviations have been compared and grouped according to the tested temperature conditions.

By grouping the Young's moduli based on the temperature at which each test was conducted, it becomes easier to observe how temperature affects the elastic properties of the materials.

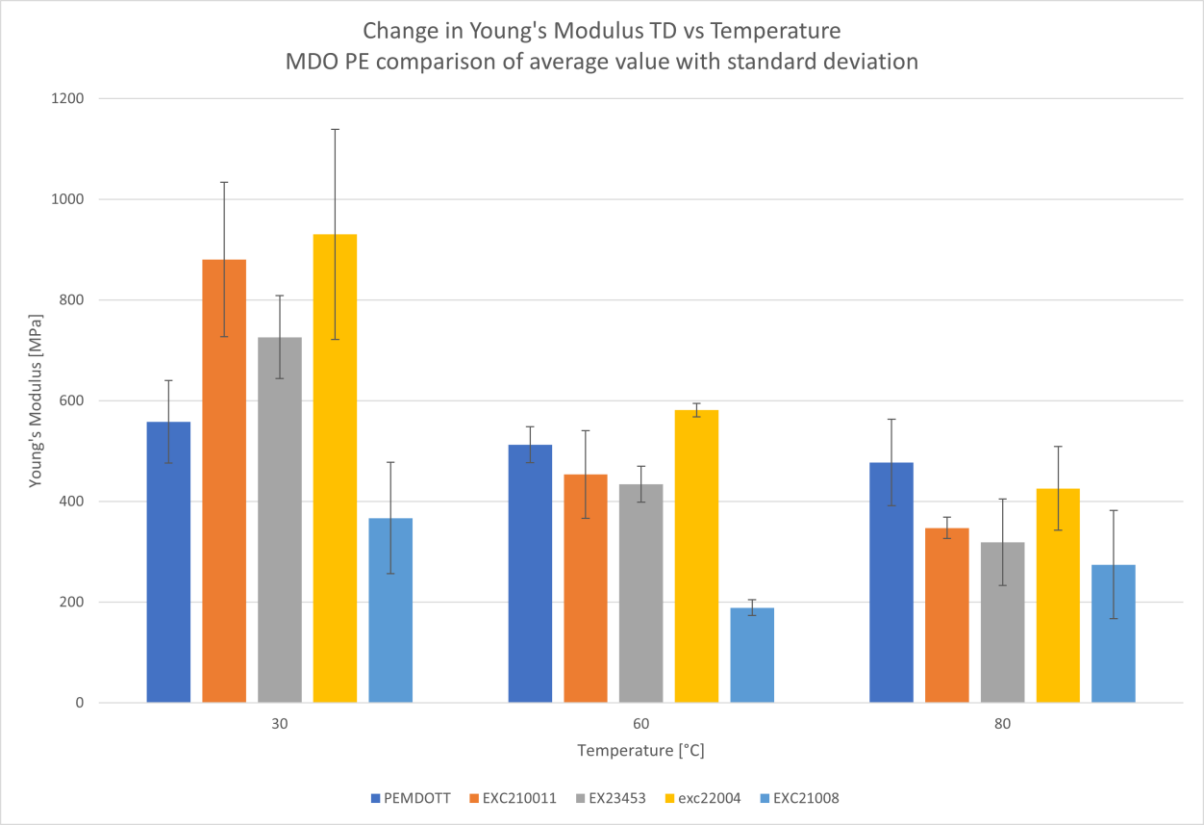

Figure 46 Comparison between Young's modulus and their respective standard deviation for only MDO PE specimens in TD

Before analysing the graph, it's important to highlight how the EXC21008 TD at 60°C appears to be an anomaly, as its Young's modulus is significantly lower than the other MDO PE, and even lower than the same measurements of EXC21008 at a higher temperature, namely 80°C. It's likely that there was an error in data collection by the machinery or in the data storage process, therefore, the EXC21008 TD at T 60°C will not be taken into consideration.

From the above graph, it's evident that in the transverse direction (TD), there is no clear winner among the tested MDO PE. Indeed, at lower temperatures, one might be tempted to say that the best MDO PE could be either EXC22004 or ECX21001, despite their not insignificant standard deviation values, which are actually larger than all other materials. However, as the temperature of the tensile tests increases, it can be seen that of all the tested materials, PEMDOTT not only emerges as the best at 80°C and the second choice at 60°C, but it is also the only one whose elastic properties are altered very little with an increase in temperature. With these considerations, the most versatile material and the one with the most consistent Young's modulus across

varying operating conditions could be the best choice, also for a factor of certainty of elastic performance in the TD direction.

The figure 56 compares the elastic moduli in the transverse direction of the MDO PE materials with those of the only BOPP tested, the MOPOTT.

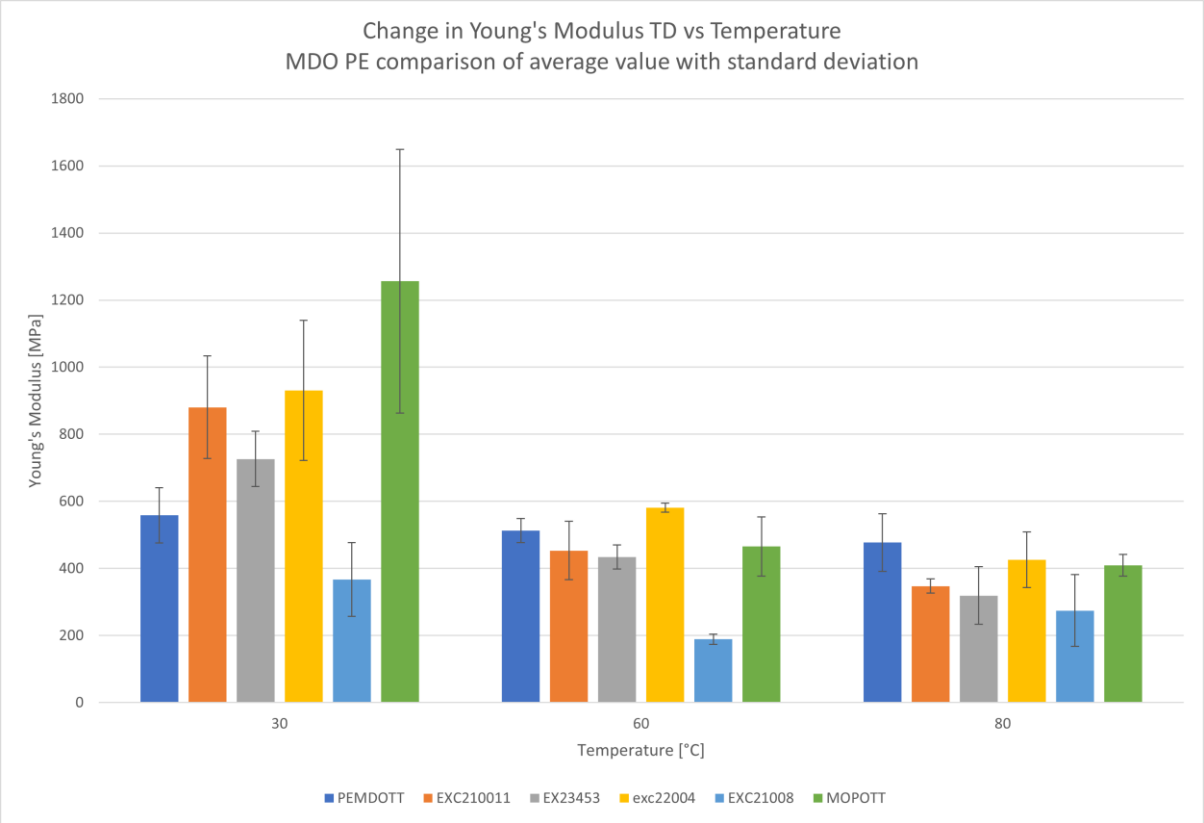

Figure 47 Comparison between Young's modulus and their respective standard deviation for MDO PE and BOPP specimens in TD

Unlike in the machine direction (MD) where MOPOTT had by far the best Young's modulus across all temperature conditions, often 2-3 times higher, in the transverse direction (TD), despite its excellent performance at 30°C, other materials such as PEMDOTT seem to better withstand temperature variations.

5 Model and data validation

5.1 Ensure the validity of the data

In this segment of the thesis, a detailed examination of the data derived from tensile testing experiments will be presented. All following considerations are related to only materials in machine direction (MD). A key point of discussion revolves around the reliability of the results garnered from the use of "dog-bone" shaped specimens tested at a speed of 25mm/min. This approach deviates from the conventional standards, specifically the ASTM D882 – 10, which prescribes a grip separation speed of 2.5 mm/min for specimens with a gauge length of 25mm. The decision to employ a higher testing speed stemmed from the constraints of limited machine usage time. A crucial aspect of this decision was the verification that such an alteration in testing conditions would not significantly skew the results.

Furthermore, this section will delve into the rationale behind choosing dog-bone shaped specimens over traditional strip specimens. This choice was predicated on the desire to maximize the efficiency of material usage, allowing for a greater number of tests with the same quantity of material. Additionally, this approach aimed to enhance the accuracy in identifying the useful gauge length of the specimens and to ascertain whether the location of breakage during the tensile tests was within acceptable bounds. The reduced length of the specimen was also crucial in ensuring the material broke within the heated chamber. With specimens having a longer gauge length, it would not have been possible to record a complete stress-strain curve. This part of the study underscores the importance of adapting testing methodologies to specific constraints while ensuring the integrity and applicability of the results.

Beginning with the shape of the samples, the data to be presented in this section will cover the Young's moduli and their corresponding standard deviations for all the materials previously introduced and discussed. All tests were conducted in the laboratories of Goglio S.p.A., under identical conditioning conditions: a temperature

of 24°C and relative humidity of 50% RH, in accordance with the ASTM D882 – 10 standard guidelines.

To discern whether the shape of the specimen had an impact, two batches of tests were conducted. The first batch used standard-sized strips with a useful length of 100mm, while the second batch employed dog-bone shaped specimens of the same dimensions as those used in the previous hot tensile tests. By setting up the experiment in this manner and using a grip separation speed of 25mm/min for both types of specimens, it was ensured that the only variable influencing the results would be the change in the shape of the specimen. This approach aimed to isolate the effect of specimen shape on the mechanical properties, specifically Young's modulus, under controlled laboratory conditions.

Table 5.1 Young's modulus at same speed using different specimen shapes

		Young's modulus "dog-bone"		Young's modulus "strips"		% difference
pemdott MD	average	1402,7	MPa	1341.5	MPa	-4%
	st dev	155,8	MPa	108.9	MPa	
exc21011 MD	average	1324,2	MPa	1412.1	MPa	-7%
	st dev	55,4	MPa	59.1	MPa	
ex23453 MD	average	1268,0	MPa	1294.0	MPa	-2%
	st dev	123,8	MPa	98.1	MPa	
exc22004 MD	average	1155,1	MPa	1332.7	MPa	-15%
	st dev	56,6	MPa	106.7	MPa	
exc21008 MD	average	977,1	MPa	1104.5	MPa	-13%
	st dev	60,2	MPa	84.2	MPa	
mopott MD	average	2706,0	MPa	2834.7	MPa	-5%
	st dev	36,3	MPa	196.0	MPa	
					average	-6%

As can be observed from the data presented in table 6.1, the percentage difference between the two tensile tests, which only differ in the shape of the specimen, appears to be minimally significant, with variations attributable to the non-homogeneity of the samples. For the materials EXC22004 and EXC21008, the percentage differences might raise some concerns, but considering the corresponding standard deviation values, there can be an overlap of the results from both tests, allowing them to be considered valid. This analysis suggests that while specimen shape has some impact, it is not significant enough to invalidate the results of the tensile tests under the given experimental conditions.

Continuing the investigation, additional tests were conducted to determine whether the non-standard traction speed used in the hot tensile tests might have influenced the results. To assess this, tensile tests were carried out using strips of dimensions as specified by the ASTM D882 – 10 standard, with a gauge length of 100mm. These tests were first conducted using the standard grip separation speed of 10mm/min, and subsequently at a speed of 25 mm/min. This approach aimed to isolate the effect of traction speed on the test outcomes, providing a clearer understanding of its impact on material behaviour under varying testing speeds.

Moreover, for each specimen, tests were also conducted at a grip separation speed of 250mm/min to determine if a rapid increase in this speed could significantly influence the Young's modulus (simulating high production speeds). Additionally, to investigate a potential opposite effect, a set of tests was arranged at a grip separation speed of 1 mm/min, exclusively for the PEMDOTT specimens. This comprehensive testing strategy was designed to explore the full spectrum of the material's response under vastly different strain rates, providing insights into how extremes in testing conditions might affect the material properties, particularly focusing on the Young's modulus under both high-speed and extremely slow testing conditions.

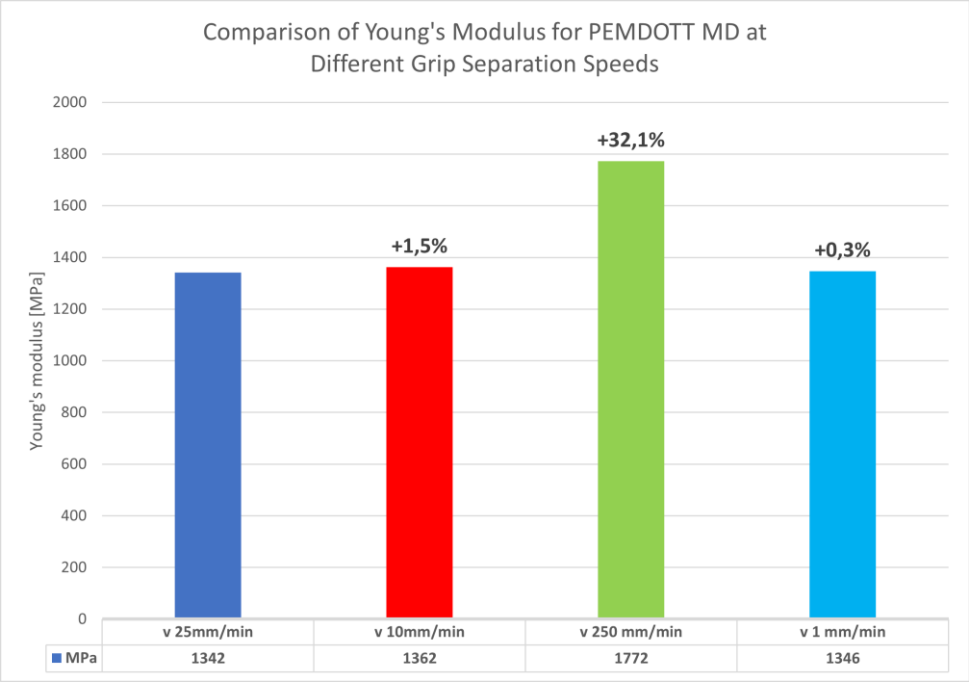

Figure 48 Young's Moduli and Corresponding Standard Deviations for Ambient Temperature Tensile Tests Using Identical Specimen Size and Shape at Various Grip Separation Speeds of PEMDOTT MD

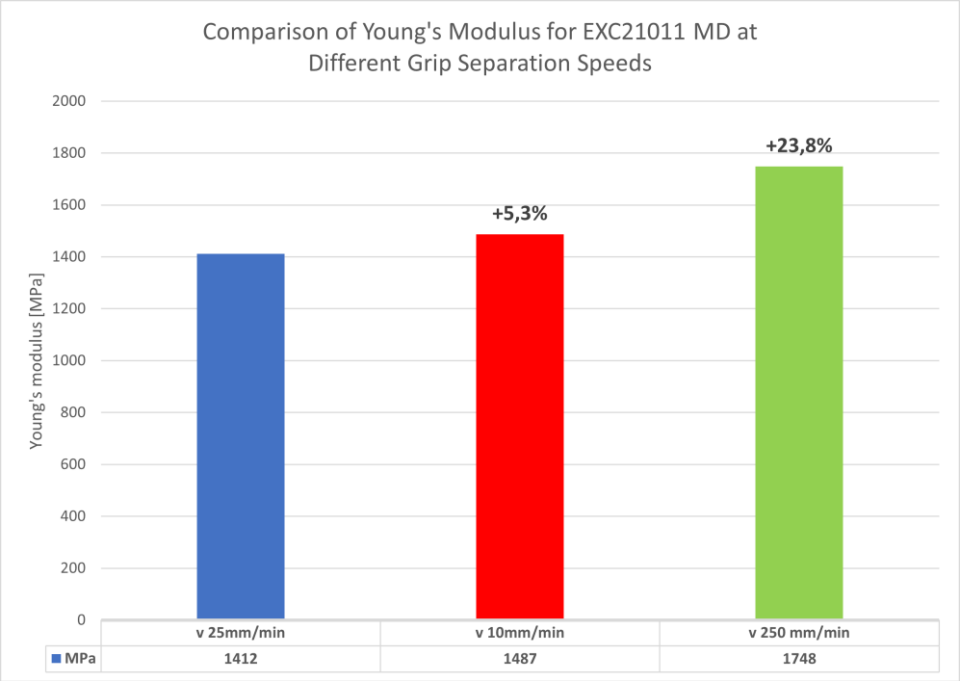

Figure 50 Young's Moduli and Corresponding Standard Deviations for Ambient Temperature Tensile Tests Using Identical Specimen Size and Shape at Various Grip Separation Speeds of EXC21011 MD

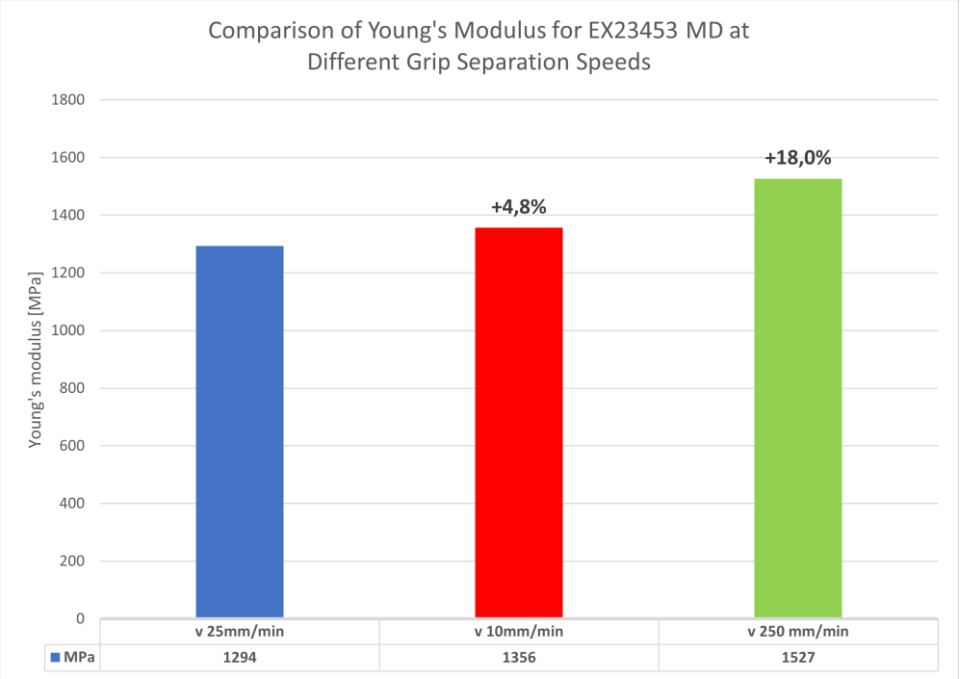

Figure 49 Young's Moduli and Corresponding Standard Deviations for Ambient Temperature Tensile Tests Using Identical Specimen Size and Shape at Various Grip Separation Speeds of EX23453 MD

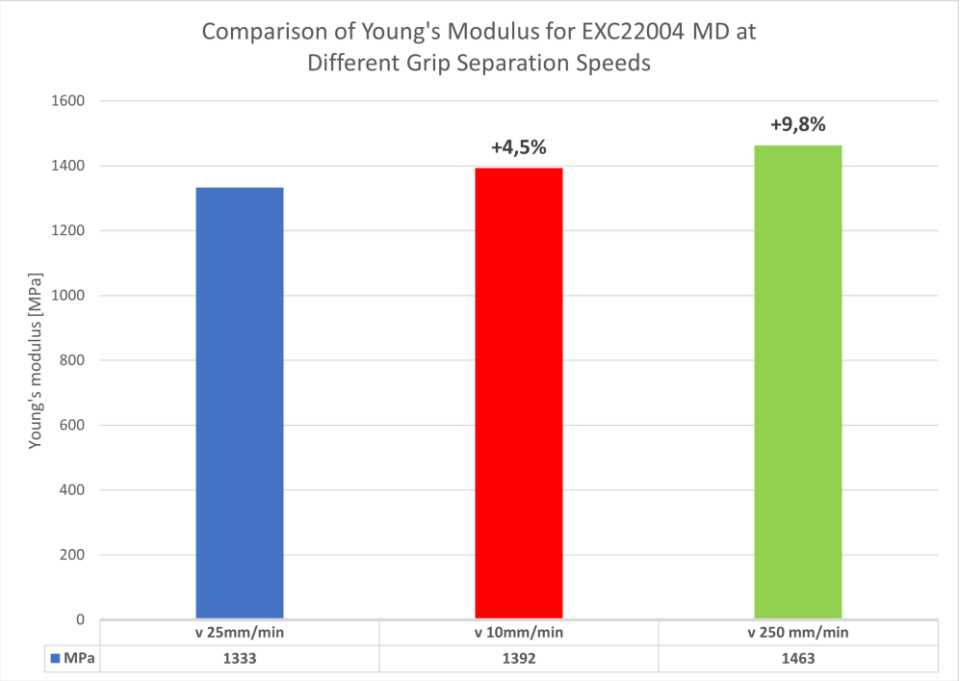

Figure 51 Young's Moduli and Corresponding Standard Deviations for Ambient Temperature Tensile Tests Using Identical Specimen Size and Shape at Various Grip Separation Speeds of EXC22004 MD

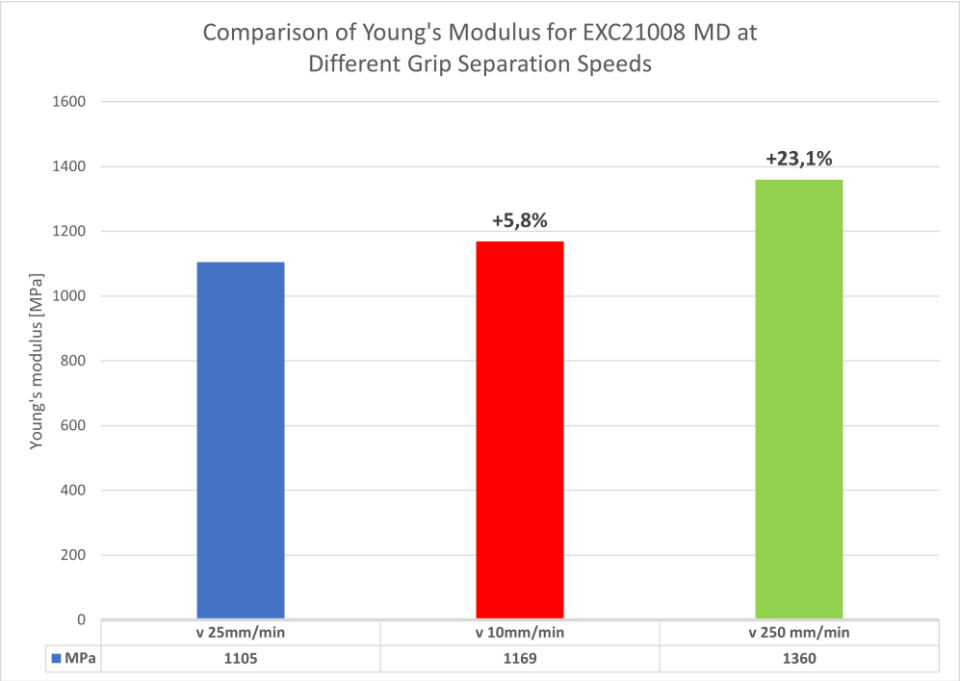

Figure 52 Young's Moduli and Corresponding Standard Deviations for Ambient Temperature Tensile Tests Using Identical Specimen Size and Shape at Various Grip Separation Speeds of EXC21008 MD

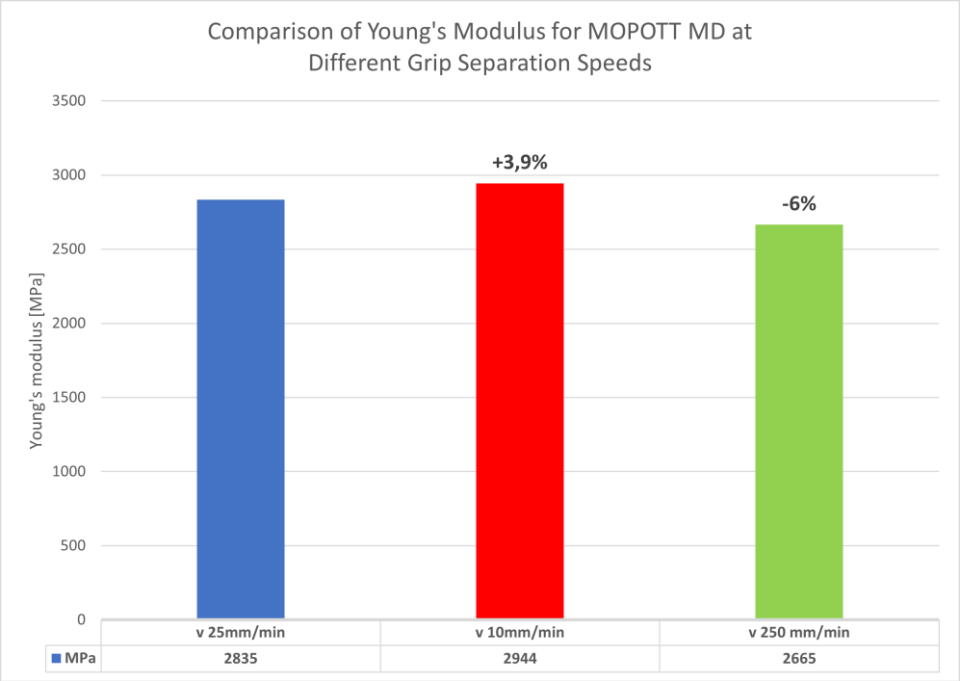

Figure 53 Young's Moduli and Corresponding Standard Deviations for Ambient Temperature Tensile Tests Using Identical Specimen Size and Shape at Various Grip Separation Speeds of MOPOTT MD

From figure 57 to 62, it is evident that the percentage difference in Young's modulus between the standard grip separation speed of 10 mm/min and the non-standard speed of 25 mm/min can be considered as having minimal influence on mechanical performance, with an average deviation slightly above 4%, attributable to other factors such as material non-homogeneity. The test conducted at a speed of 1 mm/min showed that for PEMDOTT, there is no significant difference when performing tensile tests at low speeds compared to standard speeds. Conversely, the tensile tests conducted at a speed of 250 mm/min exhibited an average increase in Young's modulus of nearly 22% for MDO PE materials, with peaks exceeding 30% for PEMDOTT. Noteworthy is the anomalous behaviour of MOPOTT, the only BOPP in the batch, which at high traction speeds showed a 6% decrease in the value of Young's modulus. This data suggests that while certain materials exhibit standard behaviour across varying speeds, others, like PEMDOTT and MOPOTT, demonstrate significant deviations, indicating the complex relationship between testing speed and material properties and an overall up trend for young's module related to higher strain rates.

The tests relating to the second round of tensile tests conducted in the company led to the conclusion that even if not under entirely standard conditions, the data obtained from the hot tensile tests can be considered reliable.

5.2 Models for predicting Young's modulus

In this section, we will present the model developed to correlate the Young's modulus values in machine direction (MD) of various materials tested with their operating temperature. Developing a model is crucial because Goglio S.p.A., with its extensive product portfolio, operates under diverse temperature conditions. These conditions are dictated by factors such as the composition of the laminate, the amount of adhesive used (measured in grams per square meter), and solvent retention values that may vary from client to client based on specific requirements. All these factors can influence the set temperature inside the ovens, and consequently, the temperature to which the material is subjected in the drying tunnel.

Creating a model based on experimental data would offer greater flexibility in case of future changes in drying tunnel conditions, changes due to different products, or alterations stemming from specific customer requirements. This approach enables the company to adapt and optimize its processes efficiently, ensuring quality and performance are maintained across varying operational scenarios.

The models proposed have been developed from the data on Young's moduli in machine direction (MD) collected during the tensile tests of the first round, namely those carried out at temperatures of 30, 60, and 80°C. Having ascertained the validity of these data in the previous chapter, to validate the models, it was decided to use as the fourth point, the data of Young's moduli collected at the company at room temperature. Despite the fact that the shape of the specimen and the speed of grip separation in most cases have little influence on the results (except at very high separation speeds), it was chosen to collect the data to validate the model by still using dog-bone shaped specimens with a grip separation speed of 25mm/min (like the one used for the previous test) in order to have data as accurate as possible.

For the development of the model, Microsoft Excel® was utilized, and various methods for data interpolation were tested. However, after careful analysis and comparison with data from existing literature, the exponential model was found to offer the best predictive capability. This approach enables a more nuanced understanding of the relationship between Young's modulus and temperature, accounting for the subtleties of material behaviour under different operational conditions.

In figure 63 a graphical representation of the results obtained:

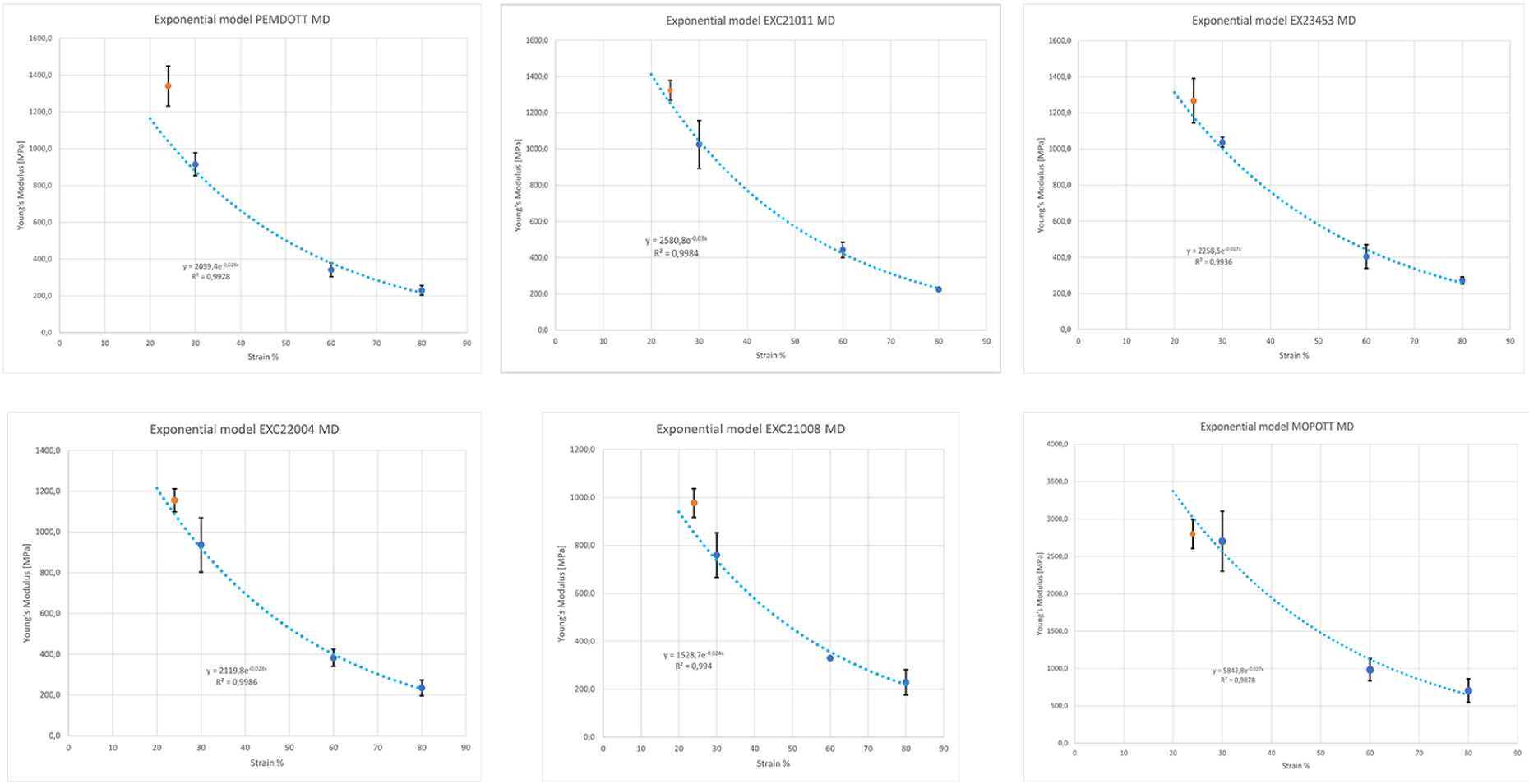

Figure 54 Graphical representation of the models developed to predict the Young's modulus (MD) value as a function of temperature for all tested materials. The blue values represent Young's moduli at 30, 60, 80°C used to construct the model, and the orange data points are the Young's moduli at 24°C used to validate the models. All data with their respective standard deviation.

The blue values represent Young's moduli at 30, 60, 80°C used to construct the model, and the orange data points are the Young's moduli at 24°C used to validate the models. All data with their respective standard deviation.

The exponential model presented in the graphs offers an insightful starting point for understanding the relationship between the elastic modulus (Young's modulus) and temperature for all the material tested. This exponential model, derived from interpolating the average Young's modulus values from tensile tests at 30, 60, and 80°C, shows a general trend that suggests a correlation between elasticity and temperature changes for most of the materials tested.

It is important to emphasize that all exponential interpolations have an R-squared value greater than 0.98. This high R-squared value indicates a very strong correlation between the predicted values from the model and the actual data points. While not definitive in its accuracy, the model serves as a useful initial framework to explore how materials respond to thermal variations. The success of this model in capturing the general trend across various materials highlights its potential as a foundational tool in material science research. It provides a basis upon which more detailed, material-specific studies can be built, especially for applications where thermal response is a critical factor. It's worth mentioning that regarding PEMDOTT, the model successfully captured the overall trend, although with less accuracy in predicting the Young's modulus values compared to the other materials. This outcome suggests that PEMDOTT's material properties might have a different or more complex relationship with temperature than the other materials tested.

In table 6.2 are the formulations of all the exponential models derived for the tested materials:

Table 5.2 exponential models derived for the tested materials where T is the temperature in [°C]

	Exponential model	R^2
pemdott MD	$2039.4e^{-0,028T}$	0.9928
EXC21011 MD	$2580.8e^{-0,03T}$	0.9984
EX23453 MD	$2258.5e^{-0,027T}$	0.9936
EXC22004 MD	$2203.4e^{-0,028T}$	0.9982
EXC21008 MD	$1528.7e^{-0,024T}$	0.9940
mopott MD	$5842.8e^{-0,027T}$	0.9878

The addition of a midpoint temperature like 45°C would have offered a more comprehensive view of the material behaviour across a broader temperature range. This could have helped in fine-tuning the model, providing a more precise understanding of how the elastic modulus changes with temperature, especially in the intermediate range that was not covered in the initial testing.

In summary, the exponential model acts as a valuable starting point for predicting material behaviour under temperature variations for both MDO PE and BOPP materials. Additionally, in the conclusions regarding all the models, it's important to highlight a significant positive aspect: the ease of implementation of this model. The last aspect is particularly beneficial in settings where complex modeling tools are not feasible or where quick estimations are needed. Its implementation in standard software like Microsoft Excel® further adds to its practicality, making it accessible to a wider range of users, including those who may not have extensive experience in advanced statistical or mathematical modeling.

Finally, knowing that the maximum acceptable deformation is 2mm per meter, it is possible to calculate the maximum force applicable to the film using the equation 5.1:

$$F = E * \varepsilon * A_{cross\ sectional} \tag{5.1}$$

Where:

- F is the force pulling the film in [N]
- E is Young's modulus calculated with the models above in [MPa]
- ε is $2 * 10^{-3}$ calculated using formula (2.4)

6 Thermal properties MDO PE e BOPP

In this section, we will explore the thermal properties of materials that have been subjected to tensile testing previously. The aim is to quantify the amount of energy needed to heat the material to the required temperatures in the drying tunnel. The set temperature significantly affects not only the mechanical properties, as discussed in earlier chapters, but also affects solvent retention, which refers to the quantity of solvent remaining "trapped" in the final laminate that has not evaporated in the drying tunnel. This aspect holds economic importance since ethyl acetate is recovered and reused within the Daverio's plant. It is also crucial for quality control, as recovering the solvent internally ensures a purer product than what is available on the market. Furthermore, there are legal and organoleptic considerations; a high concentration of ethyl acetate in the laminate could seep through the various plastic layers, potentially contaminating the food matrix inside.

Quantifying the heat absorbed by a plastic film within an evaporation tunnel presents a complex challenge. This difficulty arises from the intricate interplay between the film's physical properties and the dynamic conditions inside the tunnel. The heat absorption process is influenced by factors such as the film's thickness, thermal conductivity, and specific heat capacity, as well as the tunnel's temperature profile and air flow dynamics. Furthermore, the non-uniformity in the film's exposure to heat due to varying tunnel conditions adds to the complexity. Accurately measuring the heat absorbed requires advanced analytical methods and precise control over the experimental conditions. This complexity is a significant consideration in the design and optimization of evaporation processes in industrial applications.

As a first approximation, it is possible to quantify the amount of heat absorbed by a material by knowing its specific heat capacity, mass, and the temperature change (delta temperature) following heat absorption. This approach relies on the basic principle of thermodynamics where the heat absorbed (Q) is calculated using the formula:

$$Q = mc_p\Delta T \qquad (6.1)$$

Where:

- m represents the mass of the material measured in [g]
- c_p is the specific heat capacity measured in [$\frac{J}{g°C}$] and it's dependent mostly by the temperature of the system
- ΔT is the change in temperature due to heat transfer [K]

This formula provides a fundamental estimate but does not account for complexities such as heat transfer inefficiencies.

To better describe the dependence of specific heat capacity on temperature, analyses were conducted to experimentally quantify the values of specific heat capacity (Cp) in the temperature range of 20-100°C, which represents the extreme temperatures encountered during production. This experimental approach involves systematic measurements of c_p at various points within this temperature range, providing a detailed understanding of how the material's ability to absorb heat changes with temperature. Understanding the variation of Cp with temperature allows for more accurate predictions of the material's behaviour under different thermal conditions.

Here is an example of the tests conducted on all materials:

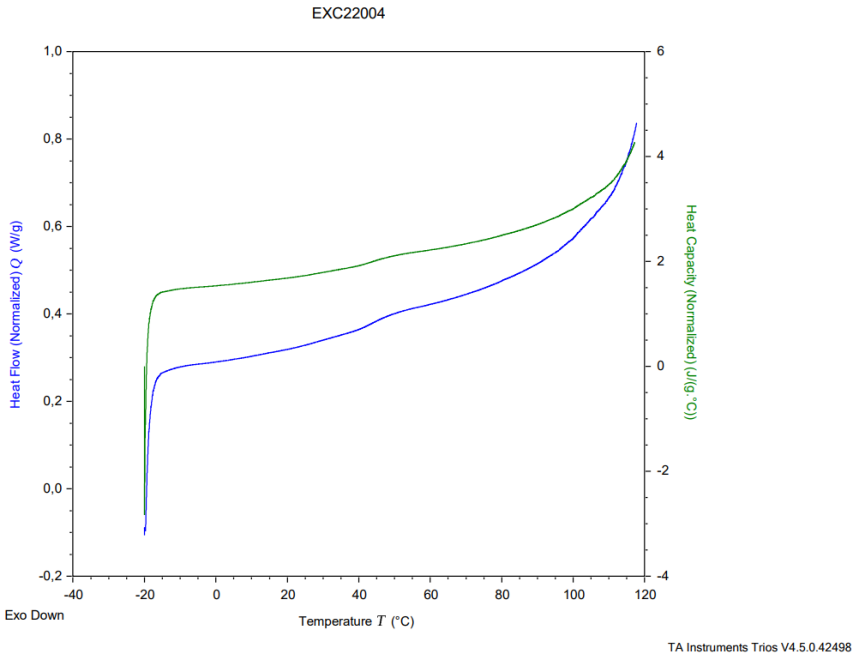

Figure 55 Example of DSC analysis for the calculation of Cp on EXC22004, also performed for all other materials

As can be seen from figure 65, the green line represents the specific heat capacity (Cp) value at different temperatures. More specifically, it can be observed that not only in

the graph shown as an example but in all the results of all the tested materials, including MDO PE and BOPP, the curve describing Cp (T) in the 20-100°C range can be very well approximated to a linear relationship. This implies that for these materials, within the specified temperature range, the specific heat capacity increases or decreases at a constant rate with temperature. For this reason, a linear regression was performed on all the Cp(T) values of all the tested materials to better describe the behaviour of specific heat capacity as a function of temperature. Below are the results of the interpolations along with their respective R-squared values.

Table 6.1 linear models of Cp obtained by interpolation of data regarding the value of Cp(T) in different temperature condition from 20-100°C

	Cp(T) linear interpolation range 20-100°C, T in [°C]	R^2
pemdott	0.0188T+1.9088	0.9854
EXC21011	0.0189T+1.85	0.9885
EXC23453	0.019T+2.4645	0.9931
EXC22004	0.0152T+1.326	0.9859
EXC22008	0.0236T+2.6854	0.9650
mopott 21008	0.0128T+2.1296	0.9943

As can be seen from the R-squared values obtained, all the linear models represent very accurately the behaviour of specific heat capacity with temperature variations in the production operating range of 20-100°C. These models allow for the calculation of the specific heat capacity of any of the tested materials at the desired operating temperature. This consideration is particularly important because, in the production of laminates with variable thickness, grammage, and solvent retention, different temperatures are used within the drying tunnel. Additionally, the initial conditions of the film before entering the oven can vary between 20°C and 30°C depending on the time of year. Having a simple and reliable model like the linear one makes it possible to calculate the specific heat capacity of the film at the temperature is expected to reach inside the drying tunnel. By also calculating the specific heat capacity at the temperature detected at the entrance of the drying tunnel, and through a simple

arithmetic mean, a highly reliable average value of the specific heat capacity can be determined for each processing operation.

$$C_{p-aveage} = C_{p-tunnel\ entrance}\text{-}C_{p-tunnel} \tag{6.2}$$

Since the relationship is linear, a simple average between the start and end points provides an extremely representative mean value. This concept hinges on the linear nature of the relationship, where changes between two points occur at a constant rate. In such cases, averaging the values at the beginning and end of the range effectively captures the overall trend. In practical terms, this approach simplifies complex calculations, making it easier to derive meaningful insights or make predictions based on the linear model.

From all the models and the analysis results, it is also possible to learn that, in general, for all materials, the specific heat capacity increases with an increase in temperature, as described by the linear models. This trend, observed across various materials, underscores a fundamental principle in thermodynamics: as the temperature of a material rises, its capacity to store heat energy also increases. The linear relationship depicted by the models simplifies this complex interaction, providing a clear and quantifiable understanding of how specific heat varies with temperature.

Finally, to conclude, a very important aspect concerns the evaporation of the solvent. Indeed, part of the energy supplied by the drying tunnel is used to increase the temperature of the material, and part is absorbed by the solvent as it transitions from the liquid to the gaseous phase. Accurately describing the solvent's transition process from liquid to gaseous phase would be extremely challenging. This is because, being a highly volatile compound, it spontaneously tends to diffuse into the gaseous phase at room temperature.

Additionally, it must be considered that the ethyl acetate is not pure but mixed with an adhesive, and therefore, there could be an alteration of the solvent's properties. This implies that the presence of the adhesive might affect the behaviour of the ethyl acetate, potentially changing its evaporation rate, specific heat capacity, and other relevant thermal properties. Additionally, a detailed investigation into the direction, flow, and speed of the air jets within the drying tunnel would be required. Furthermore, for different types of laminates, the grammage of the material varies, thus changing the quantity of adhesive per square meter applied, the desired operating temperatures, and the necessary solvent retention to pass quality tests. For the solvent as well, a highly simplified model could be proposed, assuming a grammage of 20 $\frac{g}{m^2}$ with complete evaporation of the solvent (hence zero solvent

retention), a film temperature inside the tunnel of 65°C and a starting one of 20°C, a constant specific heat of ethyl acetate at 168.94 $\frac{J}{mol*k}$ [25] and a molar mass (MM) of 88.10 $\frac{g}{mol}$. Using the same model proposed for equation 7.1, we would arrive at a result of 1735.83 $\frac{J}{m^2}$ for the evaporation of the solvent. Meanwhile, to heat the film (starting also from 20°C to 65°C), using supplier data regarding density of 0.94 g/cm³, a thickness of 0.000030m, and an average specific heat for the PEMDOTT (using equation 7.2) at 2.7078 $\frac{J}{g°C}$ [25], the necessary energy is calculated as 3436,2$\frac{J}{m^2}$.

The data obtained from the linear interpolations of the points derived from the DSC on the tested materials are in line with the data that can be found in the **literature**. More specifically, data on specific heats for HDPE in a range from 1.8 to 2.7 $\frac{J}{g°C}$ [26] can be reported, with publications showing values recorded up to 3.5 $\frac{J}{g°C}$ [27], thus in line with the collected data.

The total energy, summing up that required for evaporating the solvent and heating the plastic film, would amount to 5190 $\frac{J}{m^2}$.

It is important to emphasize that this represents an incredibly simplified scenario. This simplified model provides a basic framework to understand the energy requirements for processes like solvent evaporation and film heating. However, in real-world applications, numerous other factors come into play. These include variations in material properties, environmental conditions, equipment efficiency, and the dynamic interactions between the film and solvent. The actual energy consumption and process efficiency could differ significantly from the predictions of this basic model. Therefore, while useful for initial estimates and conceptual understanding, this model should be supplemented with more detailed analyses and empirical data for precise and accurate process design and optimization in industrial settings.

7 Conclusion

In conclusion, this thesis has extensively discussed the mechanical properties of MDO PE (Machine Direction Oriented Polyethylene) and BOPP (Biaxially Oriented Polypropylene) films, highlighting the comprehensive testing conducted in both polytechnic and company laboratories. Hundreds of tensile tests were performed at different temperatures (30, 60, 80°C and 24°C).These tests were crucial in understanding how the materials behave under stress.

The work done has not only provided valuable data to the company about the Young's modules and stress-strain curves in both machine and transverse directions. The data from these tests helped develop and validate exponential models predicting the change in Young's modulus (in the machine direction) with temperature variations. This provides a reliable tool for predicting the elastic properties of films used in production. An equally important aspect of this research has been the comparison of mechanical characteristics of similar products from different suppliers, enabling informed decisions about supplier selection based on superior mechanical properties rejecting those with inferior proprieties.

Looking towards the future, further refinement of these models is proposed by incorporating additional data at intermediate temperatures, 45°C. This step is particularly crucial for materials like PEMDOTT, where current models show less reliability.

Additionally, the thesis has addressed the thermal properties of these films. A straightforward yet efficient model for calculating specific heat for MDO PE and BOPP has been introduced, based on the linear dependency of specific heat values with temperature in the 20°C to 100°C range. This simplicity in formulation and application marks a significant advancement.

All models developed have utilized Microsoft Excel®, making them immediately applicable and user-friendly, considering the software's extensive use within the company. Moreover, a simplified model for calculating the energy necessary per unit

surface for solvent evaporation has been proposed. It is important to emphasize how the model is extremely simplified, and for more reliable results that can cover more types of laminates, further studies are necessary.

Overall, this thesis contributes significantly to the understanding and application of mechanical and thermal properties of MDO PE and BOPP films, offering practical tools and insights for industrial application. The proposed future enhancements promise to further refine these models, solidifying their reliability and applicability in real-world scenarios.

Bibliography

[1] Goglio S.p.A., «history,» 2023. [Online].

[2] Goglio S.p.A., «prodotti,» Goglio S.p.A., 2023. [Online].

[3] Goglio S.p.A., «facts and figures,» Goglio S.p.A., 2023. [Online].

[4] L. D. Nardo, «Food Packging materials,» 2021.

[5] IDFA, «Pasteurization,» 2023. [Online]. Available: https://www.idfa.org/pasteurization.

[6] P. S. Green, «Le novità proposte da Goglio a interpack 2023,» *Packaging Speaks Green* .

[7] Polythene UK Ltd, «What is MDO film?,» Polythene UK Ltd, 2023. [Online]. Available: https://www.polytheneuk.co.uk/news/products/what-is-mdo-film.

[8] Jolly Plastic S.p.A., «Termolaminazione,» Jolly Plastic S.p.A., [Online]. Available: https://www.jollyplastic.com/it/termolaminazione/.

[9] Goglio S.p.A., «Internal report Goglio S.p.A.».

[10 AVERY DENNISON CORPORATION, «Adesivi a base solvente,» AVERY DENNISON CORPORATION, 2023. [Online]. Available: https://performancepolymers.averydennison.com/it/home/technologies/adhesives/solvent-adhesives.html.

[11] Industrial Rubber Goods, «Industrial Rubber Rollers,» Industrial Rubber Goods, 2022. [Online]. Available: http://www.industrialrubbergoods.com/industrial-rubber-rollers.html.

[12] International Labour Organization, «Etil acetato,» 2018. [Online]. Available: https://www.ilo.org/dyn/icsc/showcard.display?p_lang=it&p_card_id=0367&p_version=2.

[13] Re S.p.A., «Celle di carico,» [Online].

[14] T. Iacopo, «TECNICHE DI CONTROLLO DELLA TENSIONE IN SISTEMI PER L'AVVOLGIMENTO DI BOBINE,» p. 12, 2015.

[15] Instron, «Modulus of Elasticity,» 2023. [Online]. Available: https://www.instron.com/en/resources/glossary/modulus-of-elasticity.

[16] L. Silva, «Study of the water absorption and its influence on the Young's modulus,» *Polymer Testing,* pp. 159-163, 2013.

[17] Polysack Flexible Packaging Ltd., «Top 3 Benefits of Machine Direction-Oriented (MDO) PE Films,» Polysack Flexible Packaging Ltd., 2022. [Online]. Available: https://www.polysack.com/top-3-benefits-of-machine-direction-oriented-mdo-pe-films/.

[18] J. John R. Wagner, in *MULTILAYER FLEXIBLE PACKAGING*, PLASTICS DESIGN LIBRARY, 2016, pp. 153-159.

[19] Intertek Group plc, «Tensile Properties (Sheet) ASTM D882,» Intertek Group plc, [Online]. Available: https://www.intertek.com/polymers/tensile-testing/astm-d882/#:~:text=ASTM%20D882%20uses%201,Equipment%20Used.

[20] ASTM International, «Standard Test Method for Tensile Properties of Thin Plastic Sheeting1,» pp. 1-10, January 1, 2009.

[21] PerkinElmer, Inc, «Differential Scanning Calorimetry (DSC),» pp. 1-9, 2014.

[22] Vincenzo Titone, «Effect of Moisture Content on the Processing and Mechanical Properties of a Biodegradable Polyester,» *Polymers,* pp. 5-9, 2021.

[23] M. A. a. A. Fatemi, «Tensile Behavior of High-Density Polyethylene Including the Effects of Processing Technique, Thickness, Temperature, and Strain Rate,» *Polymers,* pp. 6-12, 2020.

[24] . L. Choy, «Effect of Machine Direction Orientation Conditions On Properties of Hdpe Films,» *Journal of Plastic Film & Sheeting,* vol. 25, p. 242, 2009.

[25] M. Baluja, R. Bravo, M. Pintos, M. Paz Andrade, G. Roux-Desgranges e J.-P. Grolier, «Unusual dependence on concentration of the excess heat capacities of ester solutions in alkanes,» pp. 134-144, 1985.

[26] NETZSCH polymers, «PE-HD: Polyethylene high density,» 2023. [Online]. Available: https://polymers.netzsch.com/Materials/Details/8.

[27] H. A. B. Z.-a. M. F. T. G. M. Mahmoud Borhani zarandi, «Effect of crystallinity and irradiation on thermal properties and specific heat,» *Applied Radiation and Isotopes,* vol. 70, p. 3, 2012.

[28] Pulixin Packaging Materials (Shanghai) Co., Ltd., «PS-PP-EVOH-PE High Barrier Plastic Sheet Roll for Thermoforming,» [Online]. Available: https://www.pulixin.com/ps-pp-evoh-pe-high-barrier-plastic-sheet-roll-for-thermoforming.html.

[29] A. caravita, «MACCHINE PER IL CONVERTING: FUNZIONALITÀ E IMPLEMENTAZIONE,» p. 6, 2012.

List of figures

List of tables

List of symbols

Variable	Description
MDO PE	machine direction oriented polyethylene
BOPP	bi oriented polypropylene
E	Young's module
σ	Stress
ε	epsilon
C_p	Specific heat capacity

Acknowledgments

The first people I would like to thanks are Luca and Roberto, if I have learned so much in these months it is also thanks to them. I would also like to thank Prof. Luigi De Nardo and Dott. Osvaldo Bosetti for giving me a chance to do this internship from the very beginning. Finally, a special thanks goes to Gabriela and Andrea for sharing the hottest days of the hottest summer ever with me, doing traction tests at 80°C.